THE DESIGN AND FABRICATION OF A JOINT ACTUATION SCHEME FOR AN ARTICULATED MOBILE ROBOT

By

SHANNON RIDGEWAY

A THESIS PRESENTED TO THE GRADUATE SCHOOL
OF THE UNIVERSITY OF FLORIDA IN PARTIAL FULFILLMENT
OF THE REQUIREMENTS FOR THE DEGREE OF
MASTERS OF SCIENCE

UNIVERSITY OF FLORIDA

1995

ACKNOWLEDGMENTS

The author would like to thank the members of his supervisory committee, Dr. Joseph Duffy, Dr. John Schueller, and chairman Dr. Carl Crane for their guidance, advice, and especially patience. Dr. Philip Adsit's constant attention to detail and application of common sense are greatly appreciated.

The development of an articulated mobile robot for use in a nuclear power plant has been supported by the U.S. Department of Energy as a part of the Robotics for Advanced Reactors program.

Thanks go to the many skilled employees of the E.I.E.S. machine shop for their craftsmanship and concern for the quality of their product.

Lastly, the author would like to thank past and present CIMAR students for their input and interaction throughout his graduate career.

TABLE OF CONTENTS

Abstract of Thesis Presented to the Graduate School
of the University of Florida in Partial Fulfillment of the
Requirements for the Degree of Master of Science

THE DESIGN AND FABRICATION OF A
JOINT ACTUATION SCHEME FOR AN
ARTICULATED MOBILE ROBOT

By

SHANNON RIDGEWAY

August 1995

Chairperson: Carl D. Crane, III
Major Department: Mechanical Engineering

Articulated mobile robots have been noted for application in traversing and performing manipulation in nuclear reactor facilities. Some aspects of the articulated mobile robot that are anticipated as useful are its small cross section and its projected ability to change elevation and maneuver over obstacles. The small cross section and the loads associated with suspension of the robot while changing elevation or maneuvering over obstacles require large joint torque to weight ratios for joint actuation. A novel joint actuation scheme is described and its implementation detailed in this thesis.

The joint actuation scheme is based on a mechanism with two coupled degrees of freedom, one rotational and one translational. Both freedoms are actuated, leading to a joint with rotational and extension capacities. The design methodology presented generates a mechanism based on performance requirements. The performance requirements estimated for application to a mobile robot in a nuclear facility are utilized to develop a prototype mechanism for the evaluation of the feasibility of the joint actuation scheme. This prototype's mechanical design is evaluated. Observations are utilized to generate a second prototype mechanism for the development of multi-segment control and navigational schemes.

CHAPTER 1
INTRODUCTION

An articulated mobile robot is a type of robot that is characterized as a serial chain of segments connected by one or more degree of freedom joints. Articulated mobile robots have been examined with respect to their suitability and usefulness in the environment expected in a nuclear power plant (Crane et al. 1988, Hirose and Morishima 1990). Several characteristics of the articulated structure make it suited for navigation and manipulation in an obstacle-strewn environment with limited access. The payload capacity of an articulated robot relative to the robot's cross-sectional area would be relatively high if the payload were distributed between segments. This would enable the delivery of considerable resources to a work area within a restrictive environment. Some articulated robot concepts allow large changes in elevation and motion over obstacles.

The University of Florida, performing research for the U.S. Department of Energy's Advanced Technology Development Division, has attempted to develop an Articulated Transporter/Manipulator System (ATMS) for use in a nuclear reactor building. This effort began with Odetics, Inc. of Anaheim, California, as the mechanical design and implementation partner and Florida as the simulation and control partner. The Florida/Odetics concept consisted of 18 segments serially connected by two electro-mechanically actuated orthogonal rotational joints. Each segment was approximately 11.5 inches wide, 13 inches tall, and 24 inches long (Crane et al. 1988). Figure 1.1 illustrates the Florida/Odetics concept. Significant resources were utilized in joint design and development. It eventually became apparent that the joint actuation scheme was not feasible based on currently available electro-mechanical actuators. An effort was directed at developing and implementing a joint actuation scheme that utilized currently available technology and met design criteria derived from performance requirements. Expected transportation and manipulation tasks of the ATMS generated the performance requirements. The development of mechanical hardware would allow the implementation and validation of control schemes and simulations.

A feature of the articulated structure is its ability to make large changes in elevation. This would be useful in avoiding obstacles and in changing floors in a nuclear power plant. The main drawback of this feature is the excessive

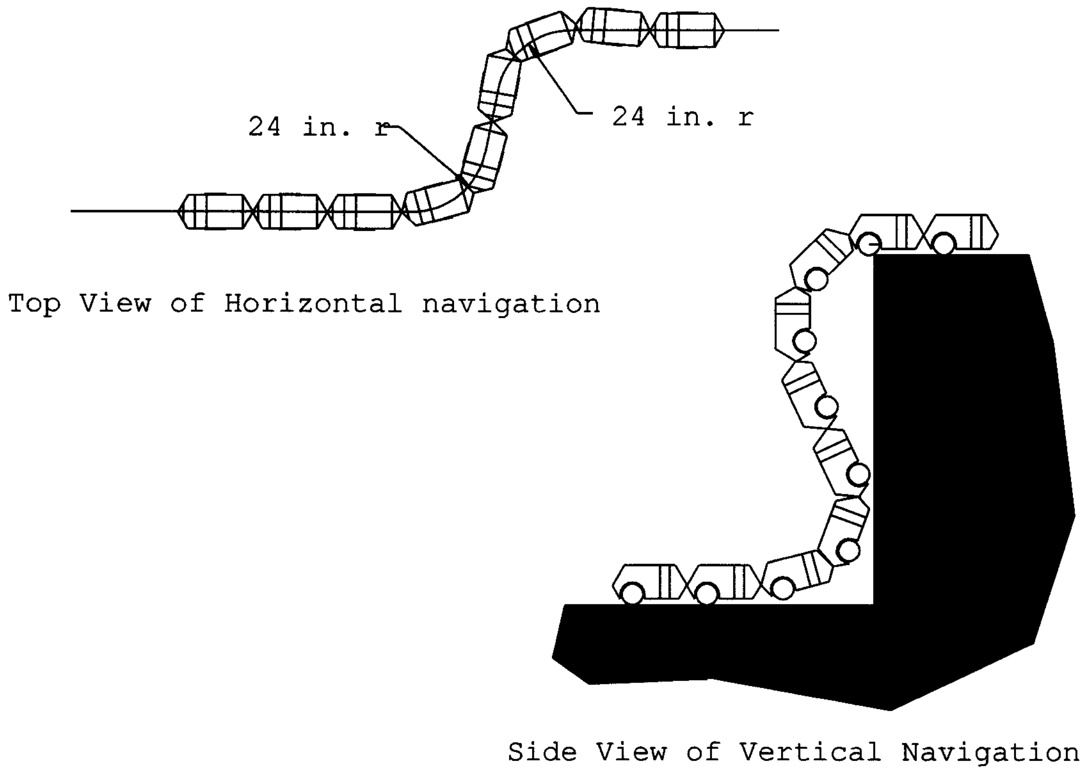

Figure 1.1 Florida/Odetics articulated mobile robot concept.

joint torque necessary to execute useful vertical navigation. This leads to large, heavy segments which in turn require more joint torque. This proved to be the limiting factor of the previous work by the Florida/Odetics team.

The effort to examine the design was begun with the intent of producing a design based on current technology that could be easily fabricated with facilities at hand. The apparent limiting factor was taken to be joint actuation. The loads expected in a joint when the articulated mobile robot is undergoing vertical navigation are by far the largest joint loads expected.

The Florida/Odetics joint actuation scheme was serial in nature. The mechanical joint between articulated segments has typically been serial in nature, that is, one decoupled degree of freedom is associated with each prime mover of the joint. This thesis details the development of a joint design methodology based on a novel parallel joint actuation scheme. The descriptor "parallel" is utilized to indicate that the degrees of freedom between two segments are coupled. The design methodology is applied to develop a two degree of freedom prototype for concept testing and then a second mechanical iteration is initiated to generate a multi-segmented articulated robot capable of vertical navigation.

1.1 Performance Requirements

Requirements were developed based on the anticipated work scope of an ATMS in a nuclear power plant type environment. The ATMS is expected to navigate to a predetermined location in the work environment, be able to perform observation while in the work environment, be able to manipulate objects in its workspace, and extract itself from the environment. The nuclear power plant environment is mostly known, enabling off-line path planning and task simulation before execution.

Two modes of navigation can characterize most expected navigational requirements for an articulated mobile robot. The first is horizontal navigation. The second is vertical-bridge navigation. These two navigational modes are illustrated in Figure 1.1. These navigational modes impose limits and requirements on the robot.

The environment expected in a nuclear power plant generates some requirements. These requirements place limits on material and component selection by dictating temperature ranges, chemical resistances required, and radiation resistance.

The following list details the requirements, the values of the requirements, and which element of the workscope necessitated the requirements. The requirements were developed in previous work concerning articulated mobile robots in a nuclear environment (Crane et al. 1988, Hirose and Morishima 1990).

1. Be capable of a radius of turn of 24 inches (horizontal navigation).
2. Ascend/descend 40° incline stairs (horizontal and vertical navigation).
3. Jump obstacles up to 36 inches (vertical navigation).
4. Change elevation up or down 10 feet (vertical navigation).

5. Bridge gaps of 12 feet (horizontal and vertical navigation).

6. Navigate in the horizontal plane at a rate of 60 feet/minute (horizontal navigation).

7. Function in a temperature range of 0 to 200° F (environmental).

8. Function in chemically aggressive environment (environmental).

9. Retain sufficient functionality during and after radiation exposure that is typically minimal except in upset conditions (environmental).

The navigational requirements are of importance in establishing kinematics, actuator selection, and structural design for the robot. The environmental requirements establish material and component selection criteria. They also impose some requirements on structural design with respect to decontamination.

1.2 Joint Concepts

Several segment joint schemes were examined qualitatively with respect to their application to an articulated mobile robot. Axial symmetry was considered. If the robot was to fall or become over turned, the ability of the mechanism to right itself is considered important. By removing axial symmetry, mechanism weight could be reduced because horizontal navigation requires less driving torque than vertical and bridge navigation. It is felt that by removing this symmetry, the robot's ability to recover after an upsetting event would be impaired.

Initial evaluation was based on examining joint actuation concepts classified according to kinematic configuration. A major criteria in examination is the joint torque generating capacity relative to overall system weight. Some of the concepts develop fair joint torque to weight relationships by reducing overall weight. Others allow for redistribution of weight while undergoing vertical navigation. A second criteria is ease of fabrication of the expected mechanical components. A third criteria is availability of "off the shelf" components. A fourth criteria is payload capacity of the concept. A fifth criteria concerns the expected workspace or reachable space of the concept. Some concepts have considerably shorter segment lengths with corresponding smaller joint range requirements but with more segments involved to reach equivalent workspaces. Several families of concepts are discussed, with one or more concept in each family detailed.

1.2.1 Serially Connected Serially Actuated Segments

Serially connected serially actuated segments similar to previous concepts were examined. Each degree of freedom of this type of joint is actuated by a single prime mover. Estimates of segment weight based on available technology indicated that this concept would be very heavy, if applicable at all to the ATMS. Kinematically, this joint configuration has several manifestations (Hirose and Umetani 1981). One can be modeled with revolute, either intersecting or non-intersecting. Figure 1.2 illustrates a joint concept based on the Hooke joint. Other configurations of this type could include prismatic joints incorporated with revolute joints.

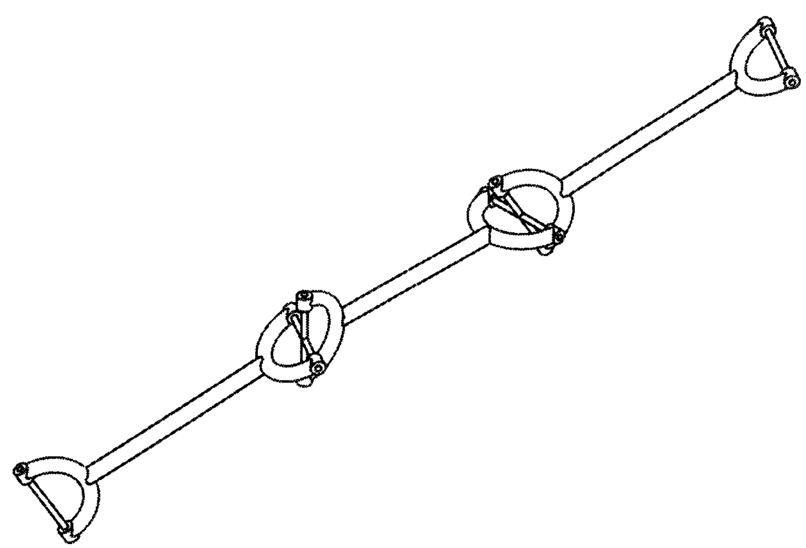

Figure 1.2 Serially connected serially actuated joint configuration.

1.2.2 Pull Cable Driven Segments

Pull cable driven segments in which a joint is actuated by tensile forces in pull cables located around the joint were examined. The joint could be something as simple as two convex bodies in contact with each other or as complex as some pull cable actuated robotic hands that have been developed. The concept offers a lightweight segment and joint but complex and heavy cable drive mechanisms that must also be transported. Sensing of robot configuration would be hampered by sliding between convex bodies and cable stretch. Load support of a structure held rigid by tensile and friction forces would be low. Figure 1.3 shows a schematic of this type of joint configuration.

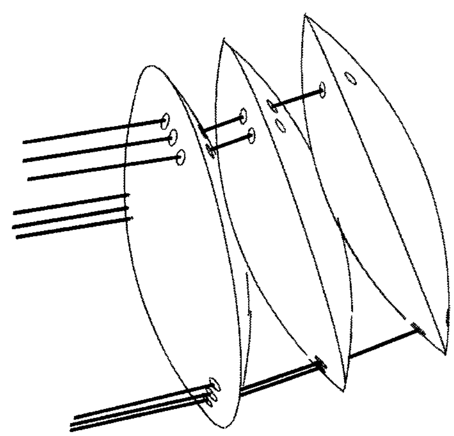

Figure 1.3 Pull cable actuated rolling element joint configuration.

1.2.3 Serially Connected Parallel Actuated Segments

Serially connected parallel actuated joints were examined. Several types with various configurations were considered. The first consisted of two joints connected by three linear actuators and one prismatic joint. Figure 1.4

schematically illustrates this joint configuration. There are three degrees of freedom between the two segments. The linear actuators are attached to each segment by Hooke joints. These joints prove difficult to design in compact lightweight versions capable of sustaining expected loads.

The linear actuator can be considered a cylindrical joint, with the prismatic freedom actuated and the rotational freedom free. One feature considered beneficial is the mechanism's ability to stretch.

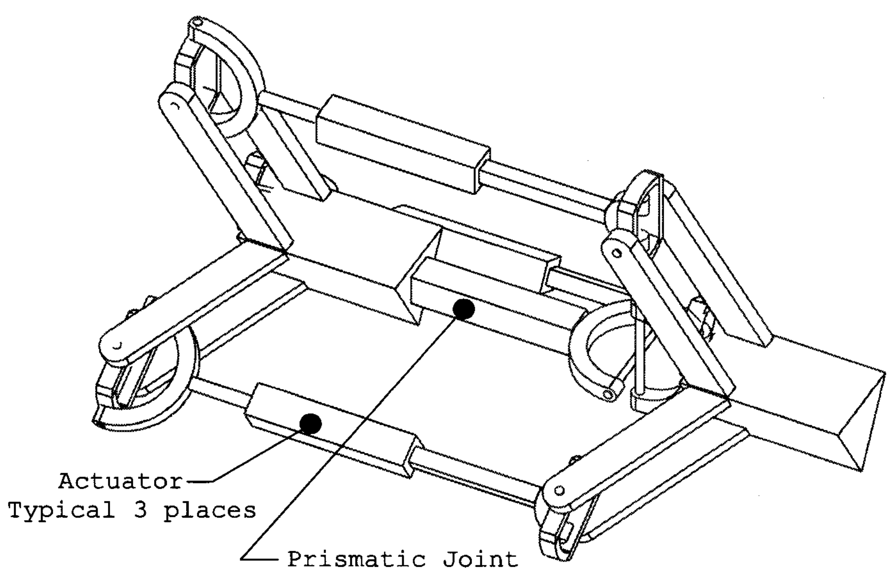

Figure 1.4 Parallel actuated joint configuration.

The necessary minimum radius of curvature of the mobile robot during horizontal navigation limits the segment length. The vertical and bridge navigational requirements relate weight per unit length to joint torque. Reduction of weight per unit length reduces required joint torque. The ability to stretch or lengthen the distance between joints for vertical navigation and to maintain the minimum length between joints for horizontal navigation is a positive aspect of this class of mechanisms.

A hybrid of the parallel and serial connections was examined in which one rotational degree of freedom was derived from a Parallel Planar Actuation (PPA). The planar nature of the parallel actuation allows the linear actuators to be connected by revolute joints. Figure 1.5 illustrates

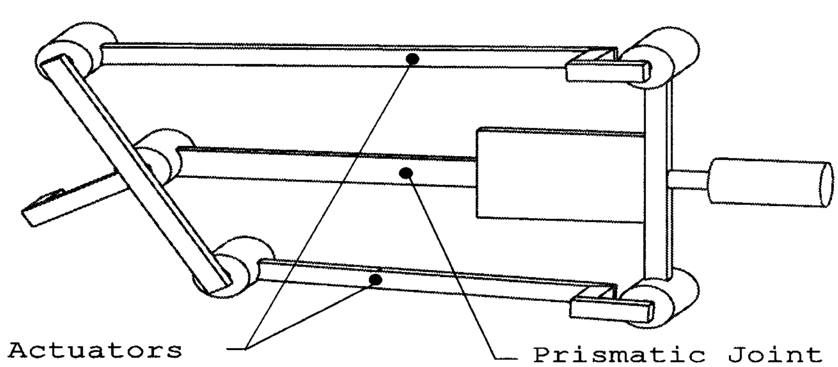

Figure 1.5 Parallel planar actuation-serial actuation hybrid.

this joint configuration. The revolute joint is much simpler to design than a Hooke joint. The serially activated revolute was determined to be a weakness because it would need to carry the moment load.

The last significant mechanism with parallel actuation is one with two Parallel Planar Actuators between joints. The planes of the PPA's are oriented at 90 degrees to each other and are acting on different segments. Figure 1.6 illustrates this joint configuration. The grounding structures for each joint make up the structure of the body.

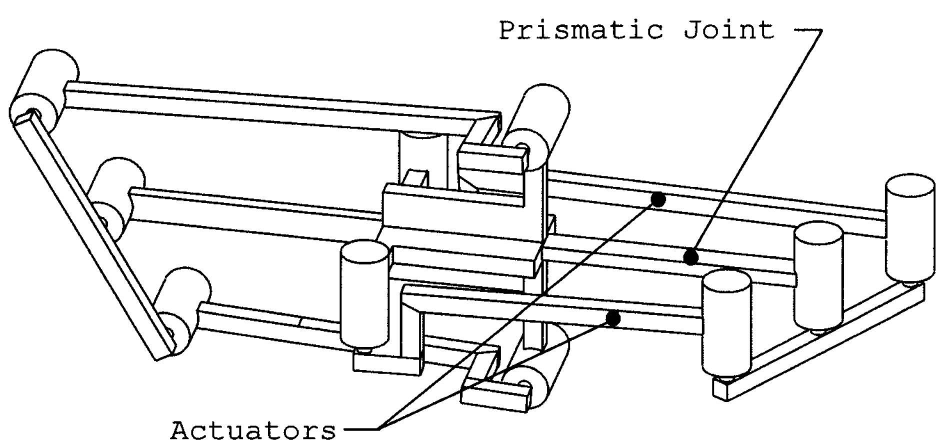

Figure 1.6 Orthogonal parallel planar joint actuation.

This configuration allows four degrees of freedom between adjacent segments. Two are sliders whose lines of action intersect and two are orthogonal rotations. The two sliding degrees of freedom allow for large changes in segment length. The planar nature of the actuation concept leads to revolute joint connections. The orthogonal rotations of a joint can intersect (Hooke joint) or have an offset. Parallel actuation gives rise to a distributed mechanism that can be both lightweight and rigid. This type of actuation introduces a sliding degree of freedom that improves performance in vertical and bridge navigation.

1.3 Literature Review

The literature available indicates that much work has been performed with respect to the control of articulated robots. Little work is presented that details mechanical implementation of an articulated robot that has more than a planar workspace. Several of the available references are discussed below. The kinematic classification of the robot is noted and the usefulness of the implementation is evaluated with respect to the ATMS.

Shigeo Hirose has implemented several articulated concepts that possess vertical plane navigation capacity. An early one is detailed in "AN ACTIVE CORD MECHANISM WITH OBLIQUE SWIVEL JOINTS AND ITS CONTROL" (Hirose and Umetani 1981). In this work, a joint activation concept that falls into the serial connection serial actuation scheme is presented. The concept consists of segments alternately connected by an oblique swivel joint and an axial revolute joint. The swivel joint axis is offset from the axis of the segment by an angle somewhat less than 90 degrees. The authors note that this joint concept is not very popular because of limited range of motion and complex control of the joints. However, they proceed to detail the development and control of a working prototype and conclude that such a device is functional as an articulated mobile robot. The authors note possible basic joint schemes and discuss the advantages and disadvantages of each. Their classification of joint type is based on mechanical joint implementation and not a kinematic joint model. They cover several serially connected serially actuated joint schemes and one parallel actuated serially connected joint scheme. The parallel actuated scheme is similar to the first one discussed under Section 1.2.3, with one of the actuators being replaced by a ball joint. They note that this type of mechanical joint is not feasible at present.

A second implementation is discussed by Hirose in "DESIGN AND CONTROL OF A MOBILE ROBOT WITH AN ARTICULATED BODY" (Hirose and Morishima 1990). This scheme removes the joint torque requirement by performing vertical navigation with a vertically oriented actuated prismatic joint. This joint is connected in series with a revolute that allows horizontal navigation between each segment. The reactions that would generate joint moment are borne by linear bearings. This implementation is a serially connected serially actuated concept that possess some advantageous properties. The primary advantage is reduction of actuator force requirements. A limitation is that the vertical navigation of the concept is limited in scope by segment height and balancing concerns. The concept results in a relatively short articulated robot with a small footprint while undergoing vertical navigation which reduces the stability of the jumping robot. The concept is adequate for maneuvering over obstacles with heights on the order of magnitude of the segment height. The concept serves to transport manipulators and sensors in a planar environment with small vertical obstructions.

The autors describe a serially connected serially actuated robot in "A SNAKE-LIKE ROBOT FOR 3-D VISUAL INSPECTION" (Lewis and Zehnpfennig 1994). The robot consists of five segments attached by two degree of freedom differential drives. This concept is similar to the one illustrated in Figure 1.2. The number and length of segments are low enough to allow electro-mechanical actuation to provide suitable performance. The vertical navigational capacities are restricted.

CHAPTER 2
DESIGN

The Parallel Planar Actuation scheme possesses several features that make it a good candidate for an articulated mobile robot. It has a sliding degree of freedom that allows reduction of weight per unit length in vertical navigation while maintaining a required minimum length for horizontal navigation. It is a parallel mechanism that can possess high rigidity with relatively low weight and it can produce large joint torques utilizing present technology.

Many areas were considered in developing a mechanism that possesses the kinematics of the parallel planar actuation scheme and meets performance requirements established for the desired application. A methodology was developed that takes as input the performance requirements for an articulated mobile robot, reduces them to those pertinent to joint design, and develops a joint design that meets performance requirements.

Figure 2.1 illustrates the principle components and geometry of a segment of an articulated robot based on the PPA concept. Two PPAs are associated with each segment.

Each PPA has two linear actuators, five passive revolutes, and one prismatic joint.

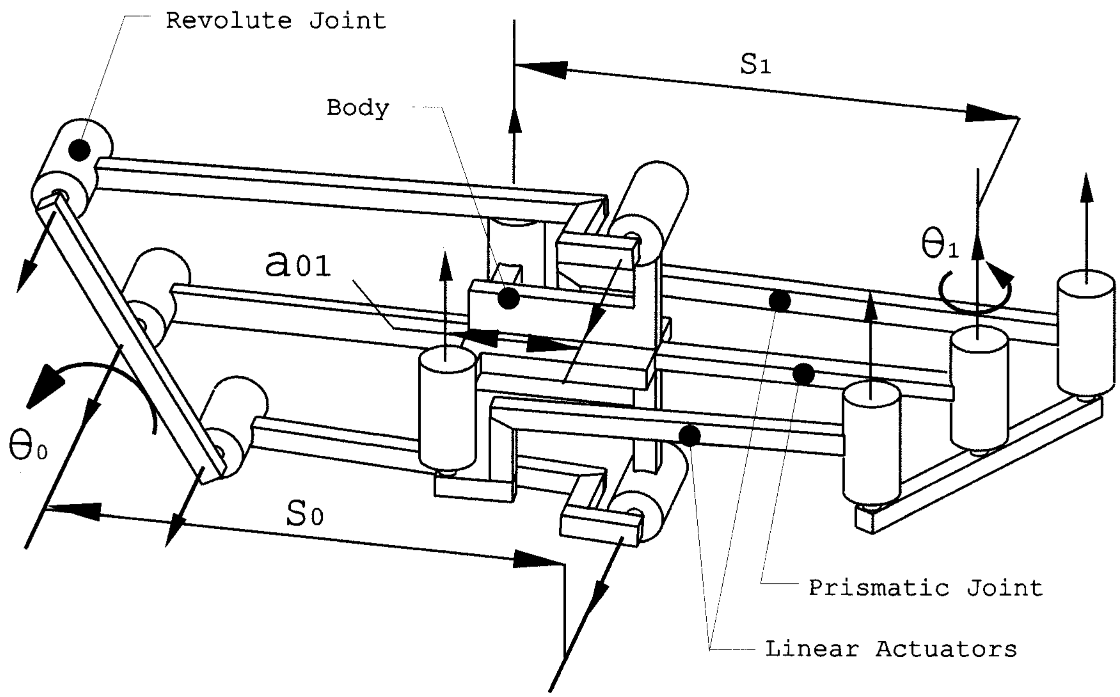

Figure 2.1 Segment components of joint articulation concept.

The design process entails specifying the mechanism constants and variable ranges based on application performance requirements, followed by generating the geometry for a suitable PPA to meet these specifications. The linear actuators, the passive joints, and the mechanical structure associated with the body of the segment and the passive prismatic joint are then addressed. The resulting design is expected to meet application performance requirements when implemented.

From Figure 2.1, the overall linear range of the segment is equal to the linear range of both the PPAs reduced by the offset a_{01}. The ATMS is expected to navigate in one plane at a time, so with respect to navigation, the rotational range of a segment is associated with one PPA, not both. This observation implies that segment length workspace requirements can be met with both PPAs but rotational workspace requirements must be met by a single PPA. Requirements that couple these two workspaces, such as the radius of turning performance requirement, require consideration of both PPAs' range of motion.

"Off the shell" components are typically available in discrete variations, sometimes with few options. For example, hydraulic cylinders are available in a limited number of diameters. Performance requirements call for exact design criteria that may or may not be met with "off the shelf" components. Best selections based on quantitative reasoning must be made in some cases. The geometry of most components is fixed outside the design process. These qualities of the design process necessitate an iterative approach where an initial design is specified, evaluated, and improved until performance requirements are met. The design methodology presented utilizes a combination of classical and computer based analysis and simulation to arrive at and evaluate a particular component and the overall design. The methodology is represented in the flow chart depicted in Figure 2.2. Each process and decision will be discussed in detail.

2.1 Mechanism Parameters

The joint actuation scheme is symmetric in the horizontal and vertical planes. The PPA comprises the symmetric portion of the joint actuation scheme. The notation detailed in Figure 2.3 is used to describe and define mechanism parameters. Mechanism parameters are a group of variables that together represent the desired functionality of the design. They are derived from component variables and generate the desired design by fulfilling the performance requirements.

The application places requirements on joint workspace and on joint torque capacity. It was assumed that velocity and acceleration requirements would be low for the high torque requirements of the ATMS. This simplifies the specification of the mechanism parameters significantly.

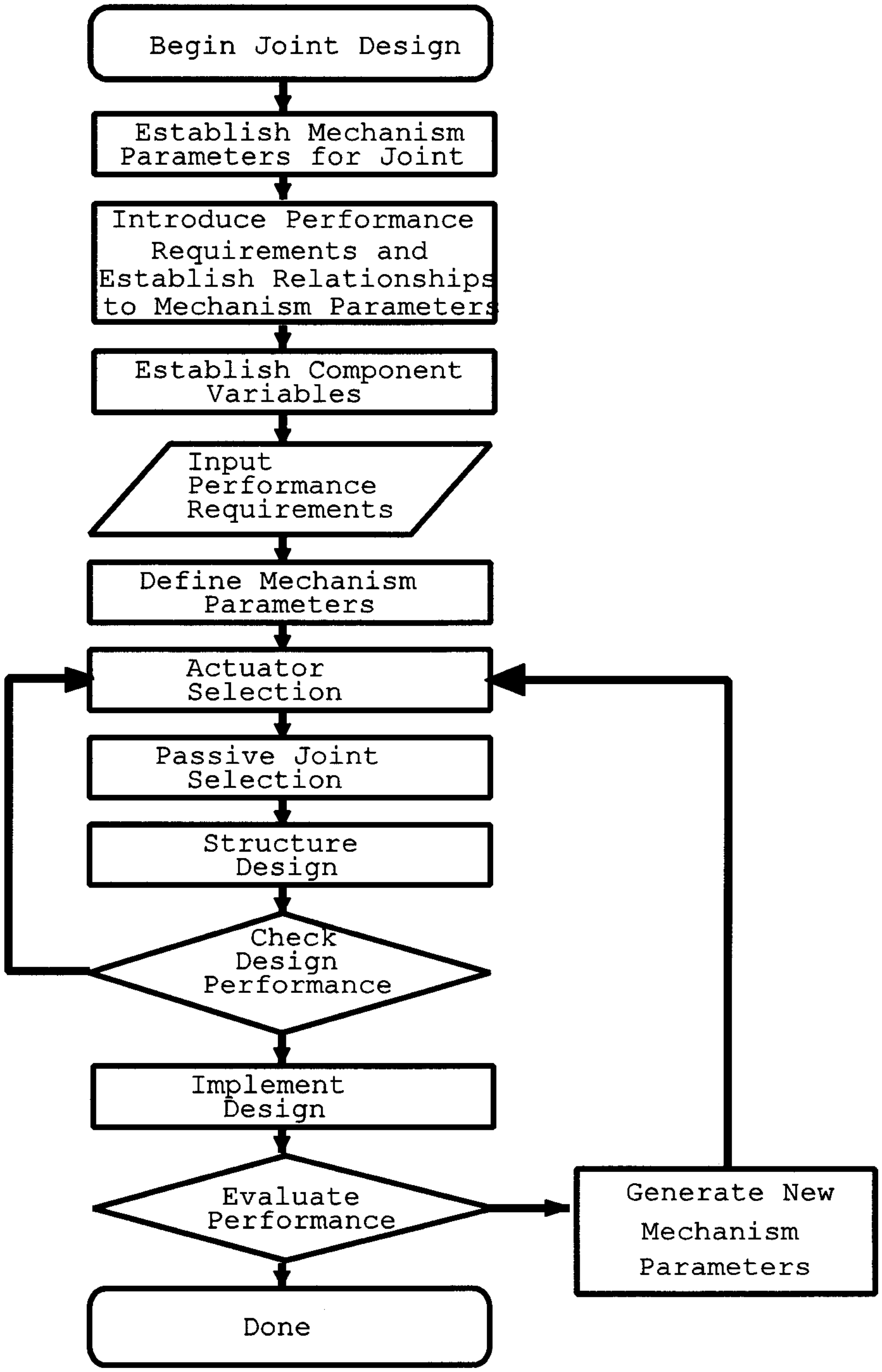

Figure 2.2 Design methodology.

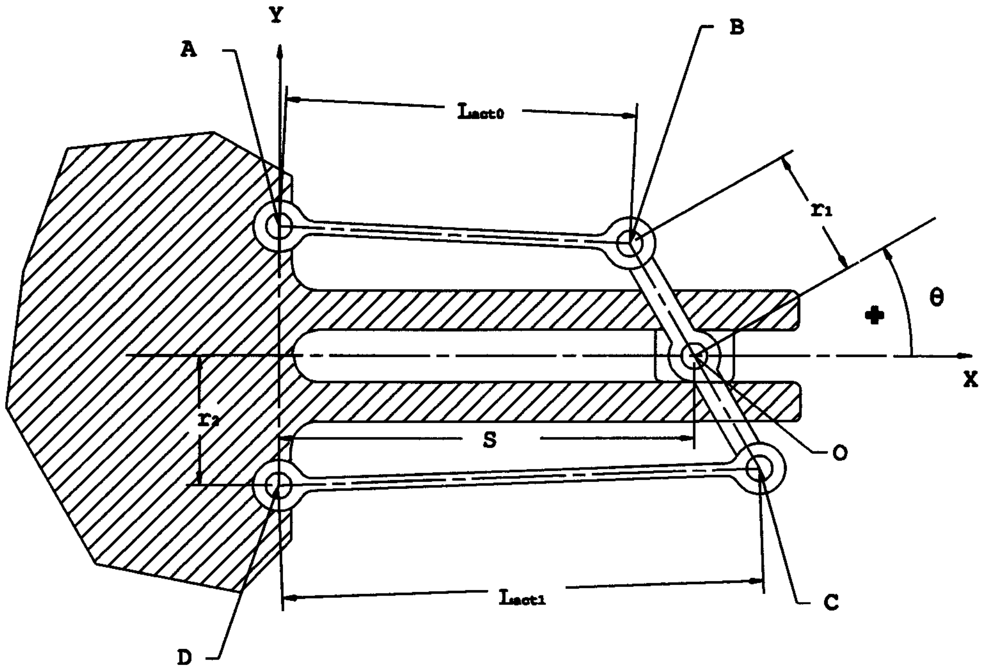

Figure 2.3 Parallel planar actuator notation.

The design of a PPA can be characterized by the mechanism parameters in Table 2.1. The parameters S and θ are coupled by the kinematics of the PPA. Joint torque is a function of both S and θ, although its dependence on S is not as strong as its dependence on θ. The statics of the PPA mechanism are developed in the Appendix. This work is utilized to develop a simulation that models the effective mechanical advantage of each linear actuator. The mechanical advantage model is based on both kinematics and statics. The magnitude of force an actuator can apply to link BC of Figure 2.3 is governed by the configuration of the mechanism, mechanism loading, and the force of its pair. If the mechanism is in static equilibrium and no external load exists in the x direction, then the components of the forces of the actuators that act along the axis of the prismatic joint must balance. The mechanism is expected to be quasi-static while undergoing vertical navigation, so static equilibrium is a good assumption.

Table 2.1 Mechanism Design.

Design Parameter	Definition
T_j	Joint Torque, range from T_{jmin} to T_{jmax}
θ	Joint Angle, range from θ_{min} to θ_{max}
S	Joint Extension, range from S_{min} to S_{max}

The configuration of the mechanism determines the relationship between mechanism parameters. Typically, the design process attempts to match the mechanism characteristics with the performance requirements. Initially, the PPA was examined with respect to matching its joint torque capacities through its workspace with the performance requirement generated criteria of high joint torque to weight ratio.

The relationship between r_1, r_2, S, and θ and joint torque was examined. The plot in Figure 2.4 illustrates variation of relative mechanical advantage over a range of θ for various ratios of S to r_1. Horizontal navigation and component interference placed limits on the selection of r_1 and r_2. Packaging concerns lead to the specification that $r_1 = r_2$. The plots in Figures 2.4 and 2.5 are for a mechanism with $r_1 = r_2 = 1.$ with the actuator force taken as 1. This relationship provides a means of predicting joint

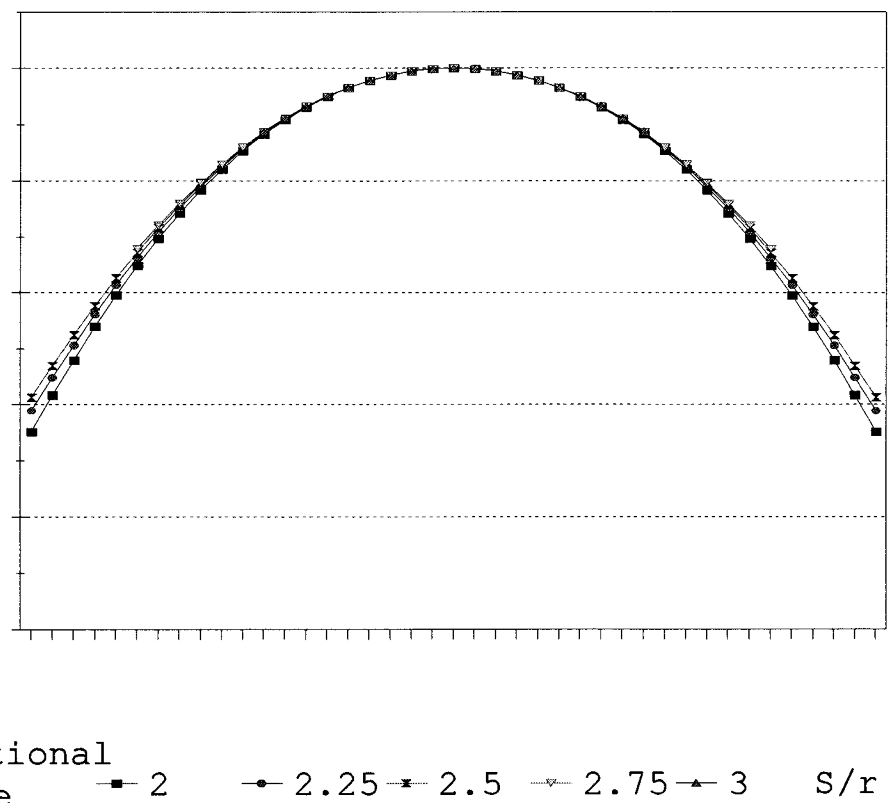

Figure 2.4 Mechanical advantage as a function of θ and S/r.

performance through the workspace of a PPA. The plot in Figure 2.5 shows the variation of joint torque with respect to S for discrete values of θ with r fixed.

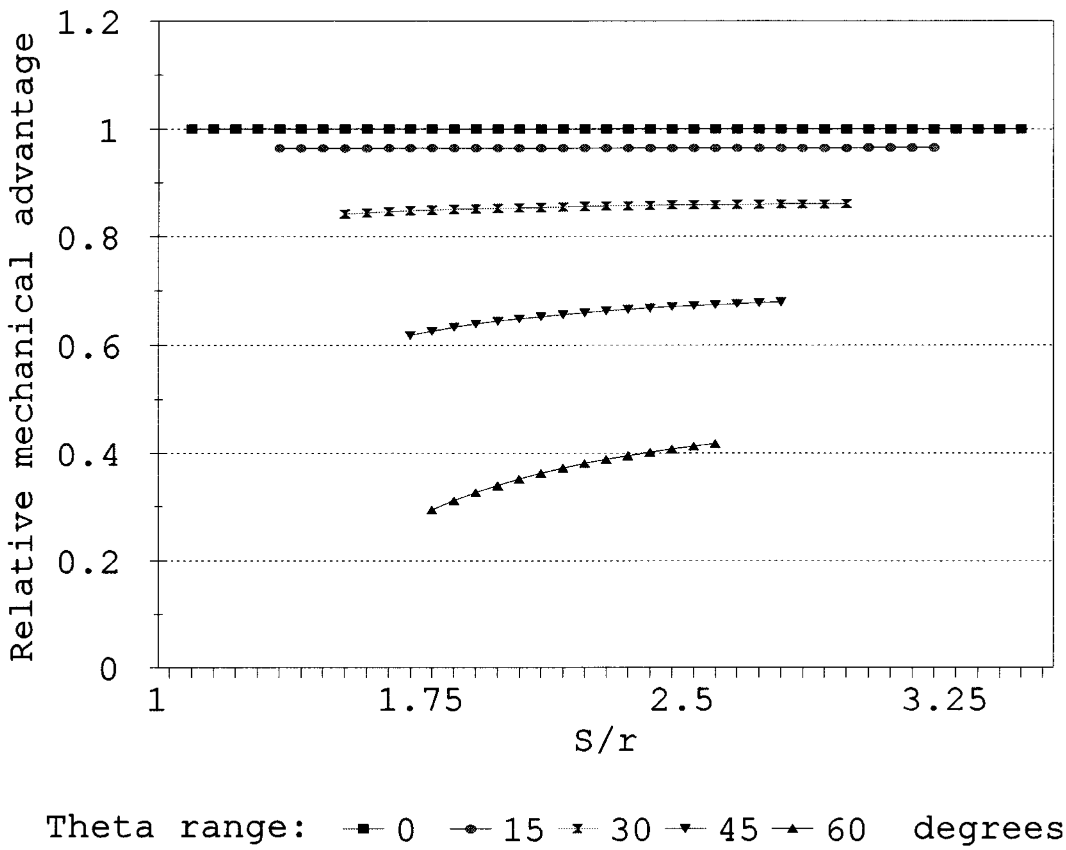

Figure 2.5 Mechanical advantage as function of S/r for various values of θ.

Figure 2.4 shows relatively no variation in joint torque as the length S of the mechanism is changed. Figure 2.5 shows substantial change in joint torque as joint angle θ is changed. The ranges of mechanical advantage are restricted to those for which the mechanism has not passed through the singularity associated with a line of action of an actuator passing trough point O (Figure 2.3).

Vertical navigation imposes large reaction moments on the articulated robot's joints. These joint loads are a function of the distributed weight of the robot and the geometry of the motion. The joint configuration in which maximum joint moment would be experienced for a given motion cannot be accurately predicted because the workscope of an ATMS is not exactly defined. This observation necessitates an assumption that the maximum joint moment occurs at the worst case for joint torque generation. This would dictate that the minimum joint torque the PPA generates be above the joint torque required. It also leads to the selection of a mechanism that maintains reasonable torque characteristics throughout its required workspace.

The weight of each segment that acts to produce the reaction joint moment can be assumed to be distributed over the length of the segment. This indirectly couples S to T_j because as S varies, the distribution of segment weight varies, affecting joint load. The design criteria S and θ are directly coupled to each other due to the kinematics of the PPA. For any S, there is a range of θ's and the magnitude of the range varies as S varies. An S exists for which θ's range is a maximum. The performance requirements of the application dictate which range of θ is most important.

2.2 Performance Requirements

Several of the performance requirements of the ATMS generate design criteria goals for a PPA utilized to actuate a joint of the ATMS. Vertical navigation requirements are expected to require the largest joint torques. The bridge gap requirement is a worst case and can easily be modeled to generate goal design criteria.

For an order of magnitude estimation of joint torques required, simple static modeling of a structure with distributed weight was performed. Figure 2.6 illustrates this model. Note the maximum landed case joint torque is 25% of the maximum cantilevered case. Using the goal of weight per unit length from the Florida/Odetics design of 4 lbs. per inch and the bridge performance requirement of 12 feet, an estimated maximum joint torque of 41,472 in.-lbs is found to be necessary during the cantilever mode of the bridge navigation.

From equations 1 and 2, it can be seen that the joint torque required is proportional to w for this type of navigation. This leads to a design goal of minimizing w_{min} to minimize joint torque required. The minimum distributed

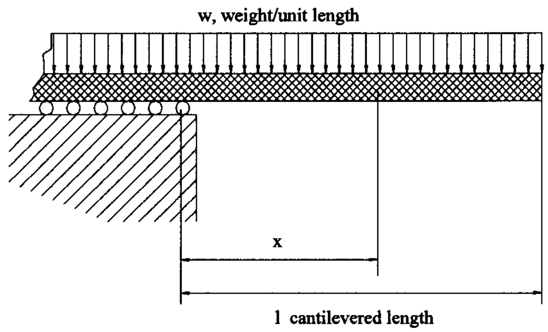

$$M = \frac{w}{2}(l - x)^2 \qquad (1)$$

Maximum at $x = 0$

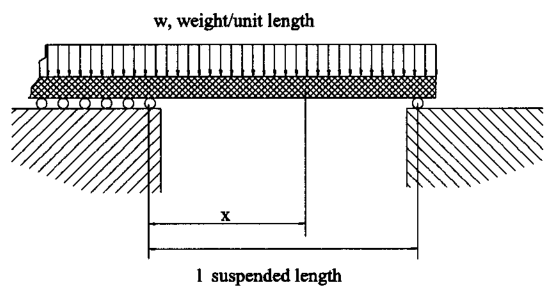

$$M = \frac{w}{2}(lx - x^2) \qquad (2)$$

Maximum at $x = \frac{l}{2}$

Figure 2.6 Joint torque estimation.

weight is a function of the weight of a segment and the maximum segment length. The maximum segment length is a function of S_{max}.

For the static case, in the vertical plane, the torque necessary to hold a rotating mass at an angular position is a function of the mass' angular displacement from the horizon. This is shown by the curve M_r in Figure 2.7. In the quasi-static case, vertical navigation of the robot will require torques that vary with angle of displacement from the horizon. Acceleration and deceleration impose other load requirements. It is assumed that high speed and accelerations will not be necessary or even desirable in vertical navigation. Joint torques in the horizontal plane arise from inertial effects and from rolling or sliding friction of the wheels. These loads are much smaller than the quasi-static loads from vertical navigation.

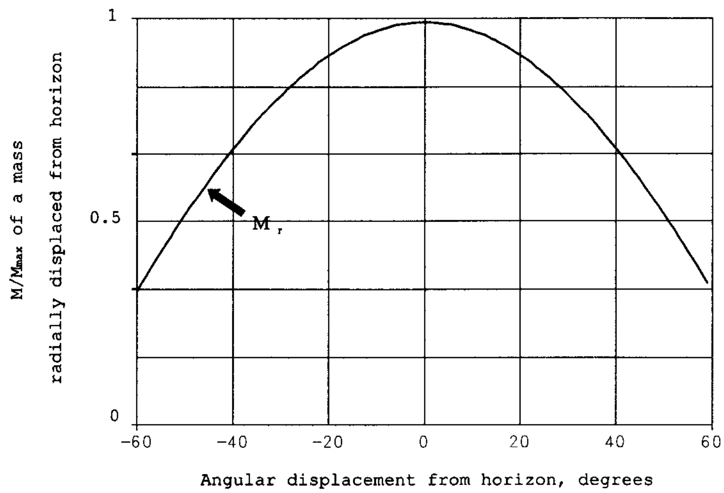

Figure 2.7 Simple joint torque requirement as a function of displacement from the horizon.

The radius of turn requirement (for the axial center line of the robot) establishes a relationship between segment length and joint range for the robot. A segment with a length and radius of turn requirement of similar magnitude would require a joint angle θ range of $\pm 54°$. The

Florida/Odetics concept had a segment length of 24 inches and a required joint range of $\pm 60°$.

2.3 Component Variables

Component variables define the performance of the components with respect to the design criteria. These are the values and functional relationships that dictate selection of components. The principle components are actuators, passive joints, and the structure of the body and passive slide. The variables that define these components are not well bounded. Some initial qualitative limitation on the range of these variables is imposed to reduce the design problem complexity.

Each PPA requires two identical linear actuators. There are two basic types of linear actuators: electro-mechanical and hydraulic/pneumatic. Electro-mechanical actuators typically utilize a rotational motor and a gear train including a screw to generate an axial thrust. Hydraulic/pneumatic linear actuators utilize fluid force inside a cylinder to push against a piston in order to generate an axial thrust. Linear actuators are specified by their force generating capacity, their speed, and their range of motion. Secondary variables are environmental hardening and fatigue life.

Actuator selection was limited to linear servo hydraulic actuators for several reasons. Hydraulic actuators capable of meeting design criteria were available "off the shelf". Electro-mechanical actuators were examined, but no "off the shelf" solution existed. It should be noted that maximum actuator torque is expected to be required while the robot is undergoing vertical navigation. The speed requirements for vertical navigation are assumed to be much less than the horizontal speed requirements. A two speed range electro-mechanical actuator that produces the same power at each speed range would easily meet design criteria, but a considerable design effort would have been invested in development. This was deemed to be a future goal of the research.

The amount of force a hydraulic cylinder under servo positional control can exert is a percentage of the maximum force the cylinder can generate under a given system pressure. The percentage is dictated by stability criteria. A rule of thumb is that optimum power transfer to the load occurs when the pressure applied to the cylinder is equal to 66% of the system pressure (Merritt 1967). Another consideration in double acting hydraulic cylinders is the different force generating capacities between push and pull strokes. This difference is caused by the reduction of piston surface area by the rod on the pull stroke.

The actuators are servo-controlled. The servo loop is effected by sensing the configuration of the PPA and utilizing this information to change actuator length in order to do useful work. Relatively few considerations directly arouse from control concerns because of the low speeds anticipated. Sensor selection, critical to control, was the most direct input to the design with respect to the control of the joint. The PPA configuration (S and θ) can be sensed by at least two methods. The first method directly senses S and θ with a rotary sensor and a linear sensor. The second senses both actuator lengths with linear sensors. Two types of sensors could be needed to effect servo control one for sensing rotary position and the other for sensing linear position. This assumes the control scheme is based on position. Absolute devices were chosen for each of these applications to avoid the necessity of a homing sequence on startup. Typical absolute sensors are more complex than their relative counterparts. For angular position sensing, the sensor type was limited to absolute optical encoders. These devices can provide the necessary resolution to accurately sense the angular position of the joint. For linear position sensing, the sensor type was limited to Linear Displacement Transducers (LDT). Other control concerns indirectly influenced the design by suggesting that friction, compliance, and backlash be minimized.

Passive joint component variables define the compliance, friction, and strength of the joint. All passive joints include some friction. Minimizing this improves load capacity and minimizes wear. The compliance of a joint, including backlash, helps determine how the joint will perform. The larger the compliance and backlash, the larger the degradation of system performance. The strength of the joint establishes the size of the joint based on expected loading.

Passive joints can be based on rolling elements or sliding surfaces, or a combination of the two. Sliding surface joints include joints in which the mating surfaces slide past each other on a fluid film. Both types of joints can be used in passive prismatic and revolute joints. When sliding element joints are used in intermittent velocity applications, a fluid film typically does not fully develop. This type of joint has relatively large surfaces of solids in contact and hence has relatively large friction associated with it. In revolute joints, the friction manifests itself on the system in the form of frictional torque. If the radius of the rotating surfaces is kept small, the frictional torque is held small. In this application, the frictional moment is proportional to the actuator thrust by the coefficient of friction μ and the bearing radius. For typical journal bearing materials, μ = 0.15 to 0.2 (Keith 1986). For a typical bearing suitable for this application, the radius would be on the order of 0.75 inches. The actuation torque generated for a given S and θ pair is proportional to the linear actuator thrust by the moment arm of the linear actuator. For a segment designed to perform approximately like the Florida/Odetics concept, the typical minimum moment arm of the actuator thrust would be 7 inches. In the worst case, the frictional moment amounts to approximately two percent of the joint actuation torque. This was deemed small enough to limit passive revolutes to journal bearings that do not in general develop a complete fluid film.

Passive prismatic joints do not possess the same advantages as revolutes with respect to friction in this application. The passive prismatic joint is expected to carry the full reaction moment load. The moment is transmitted through a couple to the body. The couple's moment arm is typically on the order of the linear actuator's moment arm or smaller due to space constraints.

The axial frictional force associated with the passive prismatic joint is proportional to the actuator thrust by μ. For sliding elements, this typically ranges from 0.15 to 0.2. For rolling elements, this μ can be as small as .0015 (Spotts 1985). Concerns about the magnitude of the frictional thrust lead to the incorporation of rolling element linear bearings in the passive prismatic joint.

The structural components are described by component variables that determine geometry and material. The geometry is specified taking into account loading, mechanical interference, thermally induced dimensional changes, and assembly/fabrication concerns. The material utilized possesses properties that are used in establishing the other component variables. These include density, stiffness, strength, fatigue resistance, and environmental resistances.

2.4 Component Design/Selection

Component design and selection is the basis of the generation of the mechanical design. The result of this section is the mechanical design of the application. The design and selection of components require an understanding of individual components. Many tools exist to aid in the analysis of components. Many manufacturers of components provide simple selection procedures based on design criteria. Several tools were developed that aid in applying the design criteria for this application to the components necessary to arrive at a design solution.

The planar parallel actuator can generate an axial force and a driving torque. The driving torque varies with angle, slide length, and specification of r. Figures 2.4 and 2.5 show the relationship of these variables over the workspace of a PPA.

As noted in Figure 2.7, the required joint torque a PPA would have to deliver when applied to an ATMS executing vertical navigation is a function of the robot's angular displacement from the horizon. The parallel planar actuator's mechanical advantage closely matches expected driving loads. This makes the mechanism well suited for the application.

These relationships allow for the sizing of the linear actuators. The loads the actuators see are the same ones the structure or skeleton of the robot undergoes. The parallel planar actuator has one non-actuated prismatic joint and five non-actuated revolute joints. Each must be designed to withstand the expected loads.

Sizing the servo hydraulic actuators requires determination of stroke length and piston surface area. The actuator length and the mechanism parameters r_1 and r_2

determine the workspace of the parallel planar actuator. The workspace limits were defined during the examination of the joint torque characteristics of a specific mechanism by evaluating the actuator length required to arrive at the location. The workspace is symmetric about $\theta = 0$. Figure 2.8 illustrates a typical workspace for a PPA.

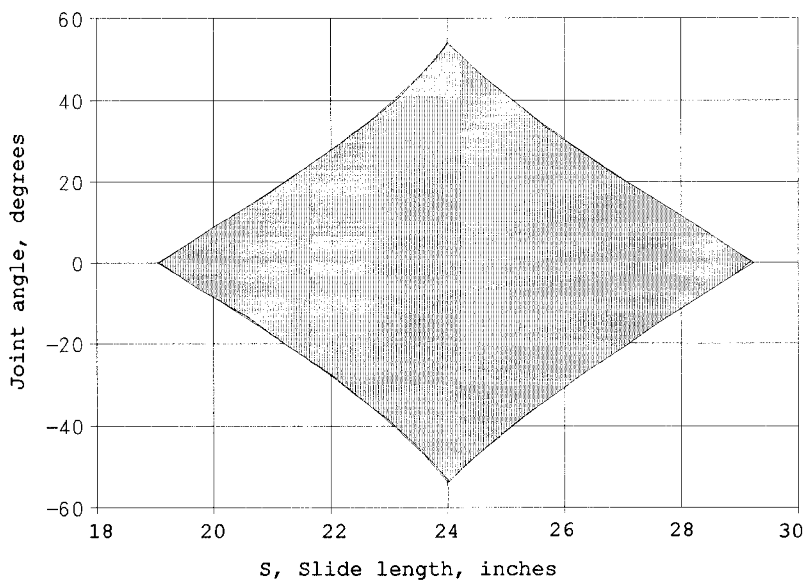

Figure 2.8 Planar parallel actuator workspace.

Design of the passive joints involves estimating bearing loads and specifying bearing configuration. The static analysis presented in the Appendix was utilized in estimating bearing loads. The linear prismatic bearings are of the recirculating ball type. A block rolls on multiple lines of balls that are rolling in grooves cut into a rail.

All surfaces in rolling contact are hardened steel. This type of bearing is specified by calculating an expected life based on loading and the wear properties of the bearing materials.

The passive revolutes were designed in bronze oilite bearing stock. This material has self lubricating properties. The bearings were designed based on projected surface area and joint loads. Material limits with respect to surface relative velocities were adhered to.

The structural components of the body and passive prismatic slide were designed based on solid modeling and finite element analysis. Solid modeling was utilized to establish assembly configuration and interference free mechanical joint motion. The finite element analysis was limited to the determination of stress and deflections in models that approximated the designed subsystems. The loading conditions were generated from the design criteria that in turn were established by the performance requirements. Design of simpler components was performed using classical methods.

CHAPTER 3
PROTOTYPE IMPLEMENTATION

Design objectives for the parallel planar actuated joint are driven by the requirements placed on it by its operational environment. Using the methodology developed in Chapter 2, a prototype implementation of a two degree of freedom planar parallel actuator was performed. This was deemed the minimum implementation necessary to evaluate the joint concept's usefulness in an articulated mobile robot. This implementation includes redundant sensors for the evaluation of two separate sensing schemes. This PPA was intended to serve as a development step for a PPA directly applicable to an articulated mobile robot.

3.1 Design Criteria

The design criteria for this application are as developed in Chapter 2. Weight per unit length, w, is to be minimized with a goal of 4 lbs. per inch. This value enables the selection of servo hydraulic actuators that meet the joint torque requirement T_{jmin} greater than 42,000 lb.-in. The proportionality that exists between w and T_j requires higher actuator force for larger weight per unit length. This design point of 4 lbs. per in. and 42,000 in.-lbs. of joint torque was the stumbling block of the Florida/Odetics concept. This point was chosen as a good starting point, realizing some deviance from it was expected. The basic geometry is expected to be similar to the Florida/Odetics concept when the robot is horizontally navigating. This concept had a segment length of 24 inches and a joint range of $\theta = \pm 60°$. The PPA provides control over both length and joint angle. The joint workspace is required to contain the joint angle range of $\theta = \pm 60°$ for a segment length of 24 inches. The slide extension S is set at the maximum that can readily be packaged in the geometry developed. The absolute maximum value of S is the full extension range of the linear actuators. The geometric parameters r_1 and r_2 were set to the largest size possible while maintaining an acceptable segment cross sectional area.

3.2 Component Selection

A 2.0 inch bore cylinder with a 1.375 inch diameter rod provides enough force to achieve the required moments when utilized in a servo hydraulic control scheme with a system pressure of 3000 psi. This cylinder has an oversized rod because it has an integral linear transducer. This allows feedback of the cylinder length directly. The cylinder was sized based on the workspace and joint torque requirements. An 11 inch stroke was found to generate a workspace and joint torque that meet design criteria goals. The stroke length is typically limited by the radius of turn performance requirement.

The joint torque plot in Figure 3.1 was generated using the moment relationships developed, maximum actuator load, and static summation of forces in the axial direction. The workspace of the joint is shown along with the variation of joint torque as a function of S and θ. The joint torque shown is for actuator 0 pulling and actuator 1 pushing, generating a positive torque. The negative torque plot is a reflection of the plot shown.

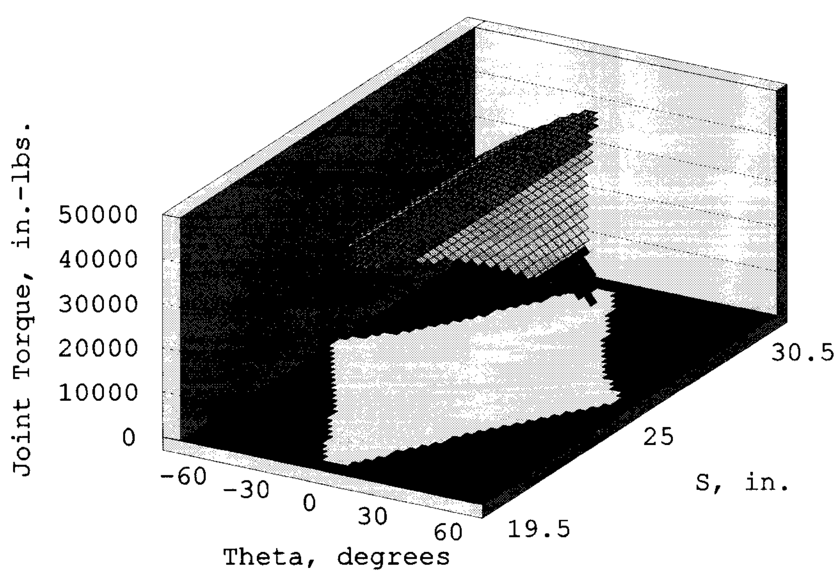

Figure 3.1 PPA workspace and joint torque characteristics.

The linear passive bearings were specified based on slide load generated by the linear actuators and the reaction moment generated by the robot's weight while it undergoes vertical navigation. Figure 3.2 depicts the variation of actuator induced slide load as θ varies for a fixed S that maximizes joint angle range. The linear bearings have recirculating hardened steel balls that roll between a rail and a bearing block. The rail is mounted to

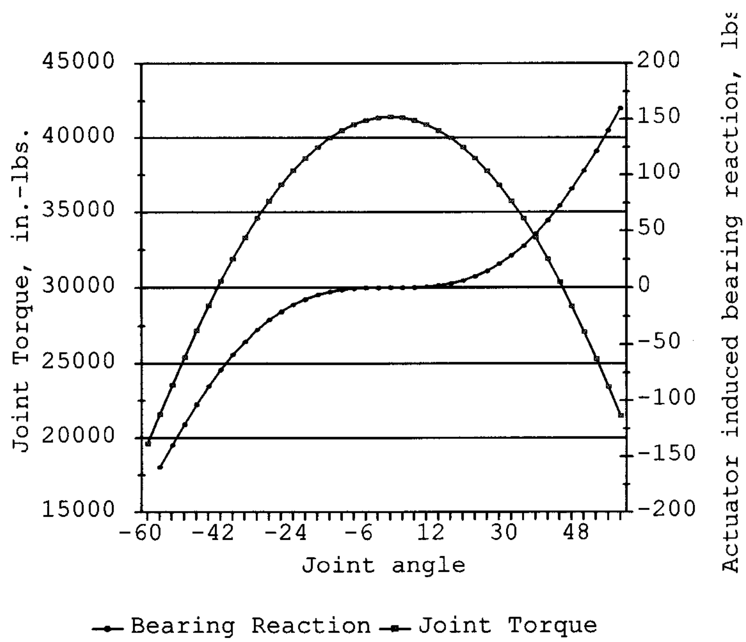

Figure 3.2 Joint torque and actuator induced slide load.

the slide structure and the bearing blocks are mounted to the body of the segment. The actuator thrust generating characteristics were utilized in designing the passive revolute joints. They were sized to have a 1.25 in. internal diameter, a thickness of 0.125 in., and a height of

1.0 in. A steel pair of trunions attached to the hydraulic actuator ride in a pair of revolute bearings. The bearing material is bronze oilite.

The structural components for the test apparatus were designed utilizing the methodology developed in Chapter 2. Each subassembly was developed utilizing IDEAS ™ solid modeling and finite element analysis, static simulation, and classical design methods. Each of the mechanical subassemblies are detailed and a brief description is given, with some analysis presented. The body is illustrated in Figure 3.3. The material used in the fabrication of the body was 6061 T6 aluminum. The body was fabricated with a machining and welding process. The welding process produced some heat distortion that had to be corrected. Figure 3.3 does not show the bearing rings and bearing caps used to fix the trunions of the cylinders in the body.

Loads on the body were estimated based on the quasi-static loads on the robot while it is undergoing vertical navigation. A worst case load scenario was deemed to be maximum actuator thrust coupled with a bearing load generated by cantilevered structure and actuator thrust. Finite element analysis modeling of the body was performed using the estimated worst case loading and approximate geometry. The geometry was restrained by limiting the

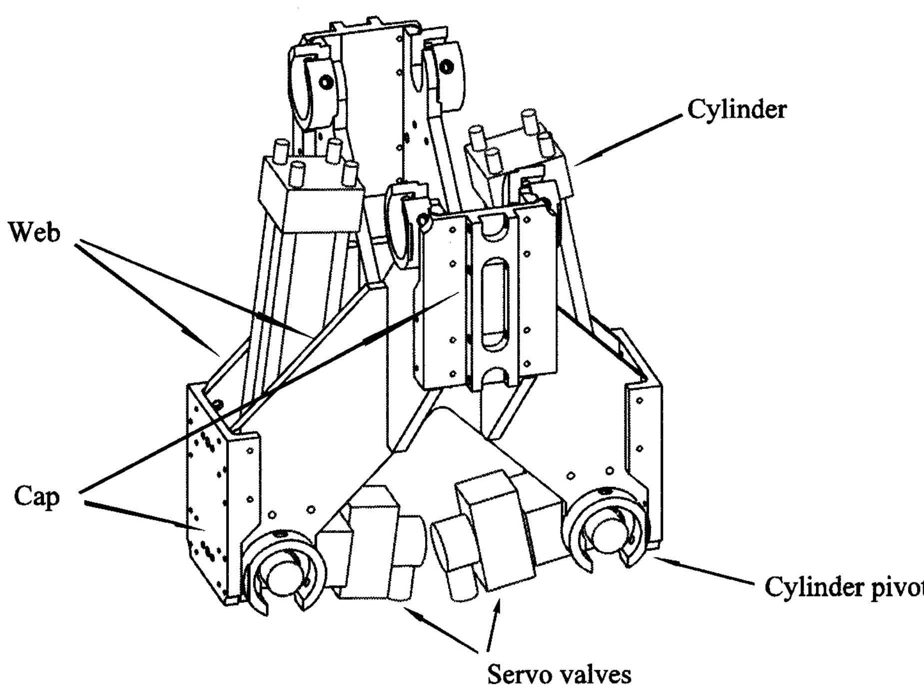

Figure 3.3 Prototype body with one pair of hydraulic cylinders.

freedom of motion at one pair of cylinder mounts to the rotational freedom associated with the cylinders and limiting the freedoms at that cylinder pair's prismatic joint to the linear freedom associated with that slide. Forces of 3500 lb. magnitude were applied to the other pair of actuator mounts in the appropriate direction. The induced bearing reaction along with the weight load of a twelve foot cantilevered section (576 lbs. for 4 lbs./in.) of hypothetical robot were applied to the bearing mounting points on the actuating PPA. Static deflections and stresses were evaluated using the analysis. A deflection illustration is shown in Figure 3.4. The deformations are scaled to be approximately 10% of the figure's width. Units are in inches.

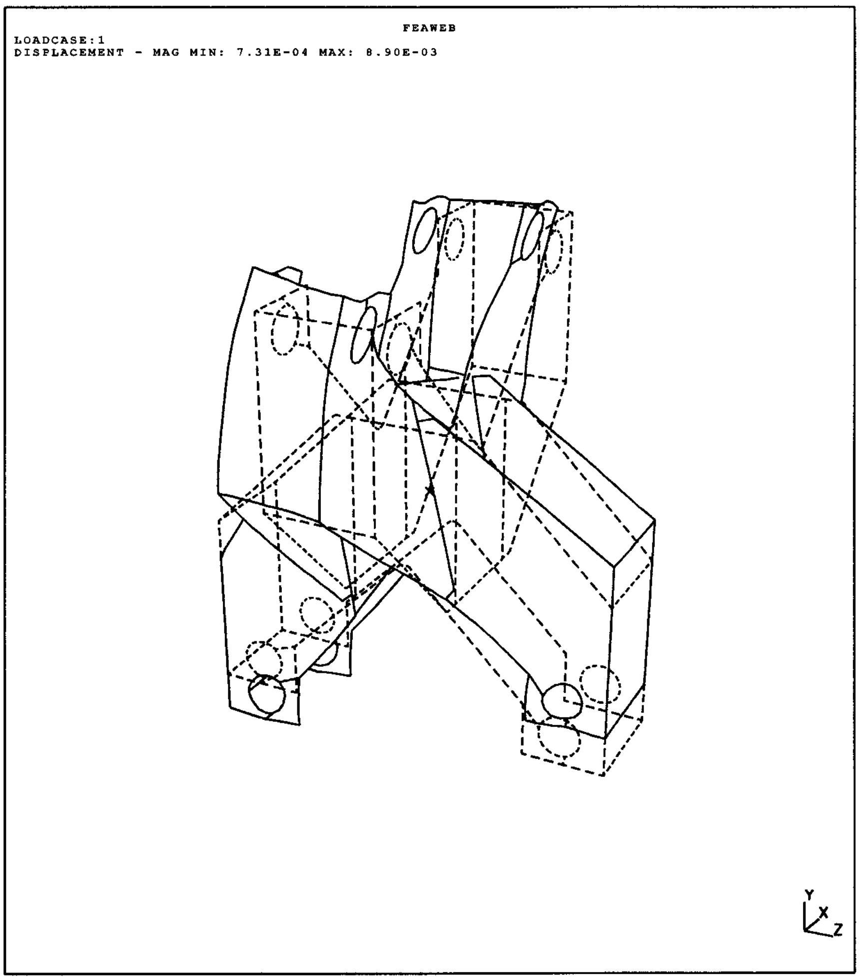

Figure 3.4 Deformation of body under expected loading.

The slide assembly is shown in Figure 3.5. The slide assembly was fabricated from 2024 T351 aluminum. There are two sets of recirculating ball bearing slides mounted in the slide assembly. These slides are induction-hardened ground steel raceways. Recirculating ball bearing blocks are mounted on the caps of the body.

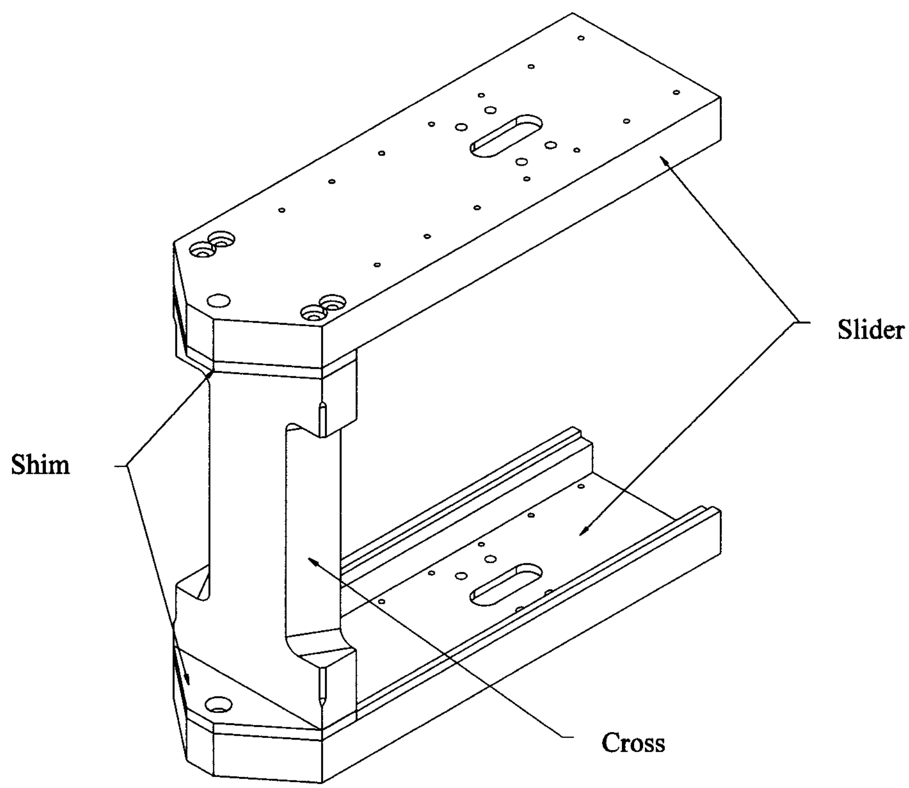

Figure 3.5 Slide assembly for prototype PPA.

3.3 Performance Evaluation

The mechanical design, fabrication, and testing of the apparatus has been performed. A photographic representation of the first prototype body with a plate attached where the ring would normally be is shown in figure 3.6. A test stand, illustrated in Figure 3.7, was designed that allowed

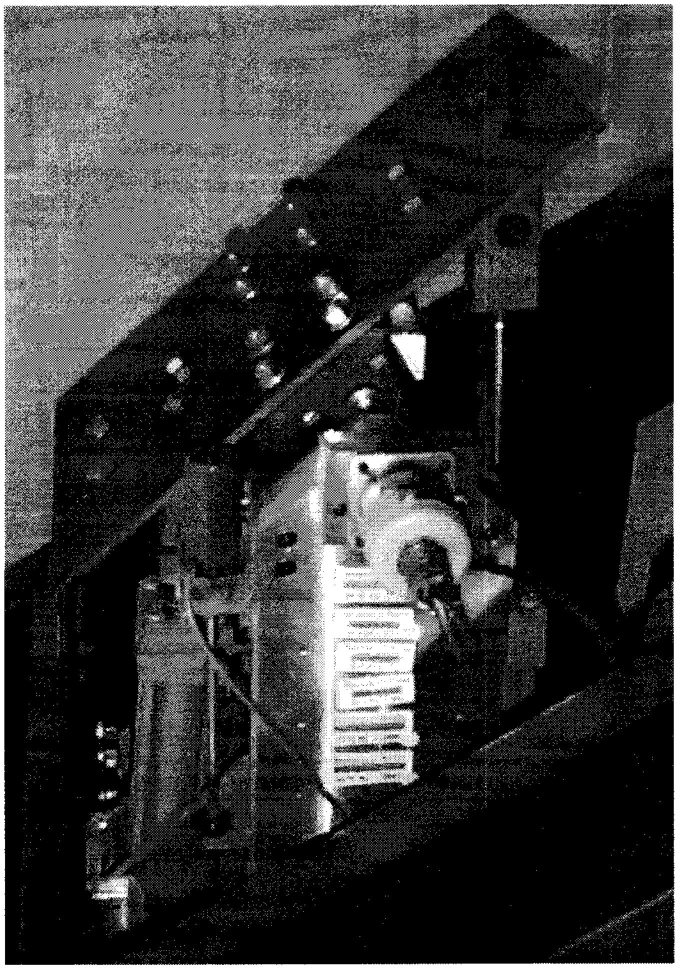

Figure 3.6 Prototype apparatus.

the body with a two degree of freedom parallel planar actuator to be tested. Loads were applied that duplicate expected loads for a segment of an articulated mobile robot undergoing vertical navigation. The test stand was fabricated from cold rolled carbon steel shapes. Its principle function is to apply a joint load that can be

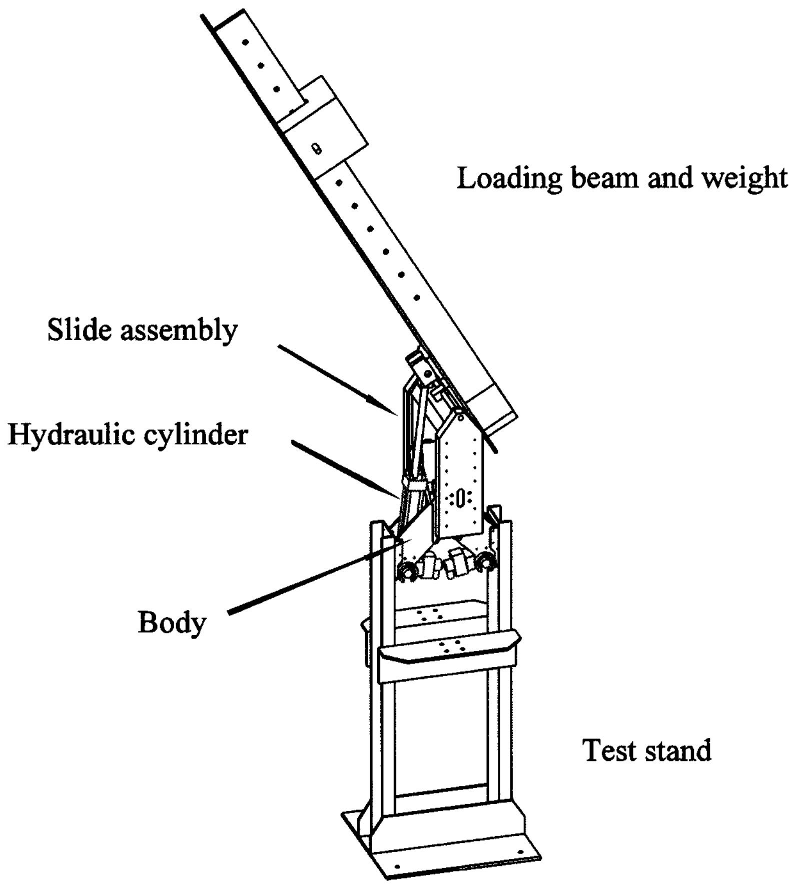

Figure 3.7 PPA test stand apparatus.

varied. The loading arm has an adjustable weight for applying moments to the actuator. The loading mechanism was capable of applying a moment on the PPA prototype over a range of 5000 to 40,000 in-lbs.

The mechanism has been operated under load through it's workspace. No mechanical failure is noted after approximately 100 hours of operation. Joint torque met calculated expectations. The test segment was controllable under load. The overall weight of a segment based on the prototype PPA (including all four actuators and both slides) is shown in Table 3.1. The ring component was not fabricated for the prototype implementation because the PPA was attached to a loading apparatus, not another PPA. The estimated segment weight, along with the maximum segment extension of 42 inches, gives a weight per unit length of approximately 5.6 lbs. per in. This figure is significantly higher than the goal of 4 lbs. per in. The joint torque required to meet jump performance requirements with $w = 5.6$ lbs. per in. is 58,060 in.-lbs. This joint torque is at or beyond the limit of control of the force generation capacity of the actuators under a system pressure of 3000 psi. An ATMS with this PPA could not meet the change elevation requirement because this requirement necessitates large joint torques and large joint angles.

Observation of the test segment lead to the conclusion that the slide has a relatively flexible mode when excited in the direction normal to the plane of the parallel actuation. The torsional stiffness of the assembly is also subject to some question. This stiffness does not come into play unless the ATMS is navigating in the horizontal plane and the vertical plane at the same time.

Table 3.1 Prototype component weights.

Part	Quantity	Weight each, lbs.	Weight total, lbs.
Body	1	39	39
Cylinder (LDT integral)	4	30	120
Slide Assembly	2	30	60
Ring (Estimated)	1	10	10
Misc (encoders, hose, etc)	1	6	6
Total			235

The manufacturing process used in constructing the first prototype created some problems with the structure. Specifically, the welding process caused significant warping of the body and lead to reworking the bearing mounts for the cylinders and slide. This lead to a modification of the slide in which its assembly was effected with shoulder bolts. This joining is partially responsible for the flexible mode the slide exhibits. It should be noted that the recirculating ball bearing slides used require two rails and two sets of bearing blocks in order to provide five full constraints. This allowed deflections between rails to affect slide stiffness, particularly in torsion.

CHAPTER 4
PROTOTYPE ITERATION

The first working prototype ATMS segment joint based on a parallel actuation scheme was completed and its mechanical design evaluated. This segment has two coupled degrees of freedom, one revolute and one prismatic, implemented with functionality incorporated for the addition of the remaining two coupled degrees of freedom. A test stand was developed so that the segment's performance could be evaluated under load. Observation during testing lead to recommendations for improvements in segment design. Fabrication also produced some suggestions for modifications.

The first prototype enabled the evaluation of the PPA as a joint actuation scheme for an articulated mobile robot. It also served as a platform for the development of control algorithms for the joint actuation scheme. Following the goals of the project, a second prototype design was undertaken that would lead to hardware capable of performing multi-segment planar navigation. The navigational plane was to be determined by the mounting apparatus. Much knowledge was gained in designing and implementing the first prototype. Several design criteria were relaxed in the first prototype that were necessary for the performance requirements of vertical navigation of an articulated mobile robot in a nuclear environment. A design and implementation iteration was deemed necessary in order to incorporate new design knowledge and to consider relevant performance requirements.

4.1 Design Criteria

These observations and those noted in Chapter 3 were considered during the development of the design for the second prototype segment. Two main design criteria goals developed from the observations. One is reduction of w and the other is increased slide stiffness. These are obvious, but necessary goals. The design criteria are left as originally stated in Chapter 3. The concessions made in the first prototype to enable sensor scheme testing and rapid structural prototyping were to be reduced or eliminated. Attention was to be paid to systems integration including consideration of cable and hose paths.

4.2 Component Selection

With both goals in mind, material selection was reevaluated. The first prototype segment is primarily aluminum. There are fiber reinforced plastics that possess significantly better stiffness to weight ratios than does aluminum. The initial concern with these types of materials is whether they conform to the environmental performance requirements. A second concern is manufacturability.

Environmental effects on composites can be looked at in several categories. Thermal, chemical, and radiation effects are three generally accepted categories. The thermal environment of the ATMS is expected to range from 0° to 200° F. The chemical environment is relatively unknown, but not expected to be aggressive. The radiation environment is also unknown, and is of the most concern. Under general operating conditions, exposure is expected to be minimal. However, the ATMS is supposed to handle upset conditions, and in these cases, radiation exposure is expected.

The literature was surveyed to investigate radiation damage to fiber reinforced polymers. It was found that glass does not make a good reinforcing phase due to boron impurities (Clough et al. 1991). Carbon is a favorable reinforcing phase, with respect to its radiation hardness. For reasonable temperature ranges, a carbon/epoxy composite retained or increased its mechanical properties when exposed to 1×10^{10} rad (Milkovich et al. 1988). This exposure level is on the order of exposure that is lethal to most hardened electronic hardware. Carbon fiber also has a very good stiffness to weight ratio. Aluminum's stiffness to weight ratio is approximately 1×10^8 in and carbon/epoxy's is approximately 2×10^8 in. (Askeland 1984).

Manufacturing a composite body for the ATMS poses some difficult problems. These are primarily associated with mechanical fasteners and dimensional tolerances. Machining is possible, but the composite is isotropic by nature and machining can give rise to large stress concentrations that induce interlaminar failure. Volumetric changes of the matrix during processing can give rise to dimensional changes. With these limitations in mind, a manufacturing process was devised that minimizes dimensional changes and allows holes for mechanical fasteners to be molded into the part. The process is based on the wet lay-up method, utilizing either a vinyl ester resin (a modified epoxy resin) or an epoxy resin. It could be adapted to a preimpregnated composite if needed. One attractive feature of the process is that it uses a mold that can be used more than once. This allows identical parts to be made inexpensively. The primary cost is for the mold and can be spread out over several parts. The material and labor in each part is significantly less than that involved with a conventionally manufactured aluminum part. This does limit design modification, so care must be taken in designing the initial mold.

The body has been changed from an internal to an external structure. This was done to increase torsional rigidity, increase internal component protection, and allow redesign of the slide assembly to improve stiffness. The external body configuration also lends itself to manufacturing processes available for fiber reinforced plastic. The geometric parameters r_1 and r_2 were maintained at 6.25 inches

The slide structure has been augmented by the selection of linear bearings with bearing blocks that each provide all five constraints. This allows more direct load transfer to the slide structure from the body. The orientation of the bearings has been modified to improve stiffness.

The actuators of the second design segments are 2 in. bore 11 in. stroke servo-hydraulic actuators without integral linear displacement transducers (LDT's). Linear displacement is measured via a LDT mounted between the body and slide. The actuators, along with the geometry of the structure, lead to an implementation of a PPA that possess the workspace and joint torque generating capacity shown in Figures 4.1 and 4.2. Figure 4.1 shows the workspace of the joint with respect to S and θ and the estimated maximum joint torque capacity for each point in the workspace. Figure 4.2 shows the maximum joint range and the associated actuator induced slide load.

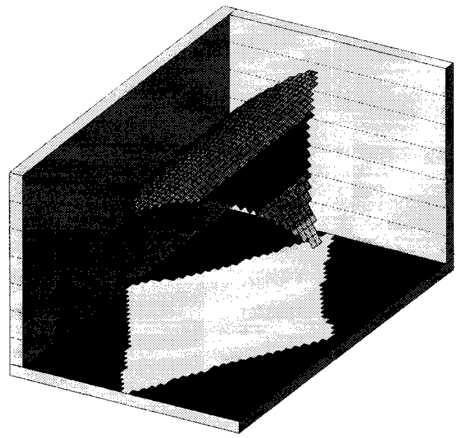

Figure 4.1 PPA workspace and joint torque generating capacity.

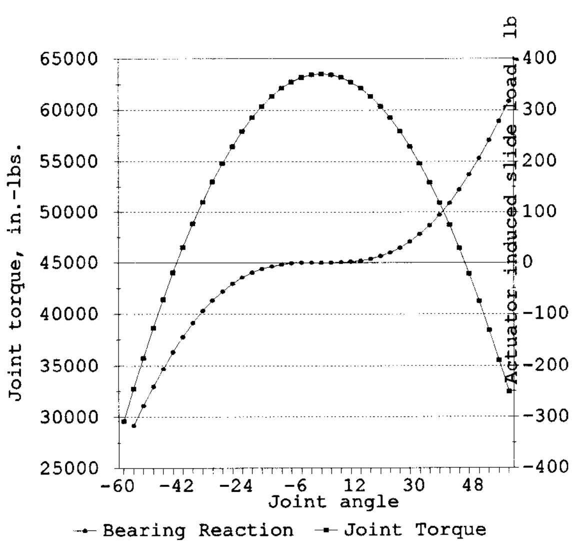

Figure 4.2 Joint torque and actuator induced slide loads of PPA.

Figure 4.3 illustrates two linked segments of the ATMS composite design revision. Figure 4.4 illustrates a sectional view of one body. The slide configuration is shown, along with actuator mounting details. Several major parts are broken into assemblies of smaller parts to facilitate assembly. The slide is the most notable of these. It is separated into four components that are assembled with threaded fasteners. Actuator mounts have been designed and fabricated. These are complex carbon fiber composites with bronze bearing surface inserts and

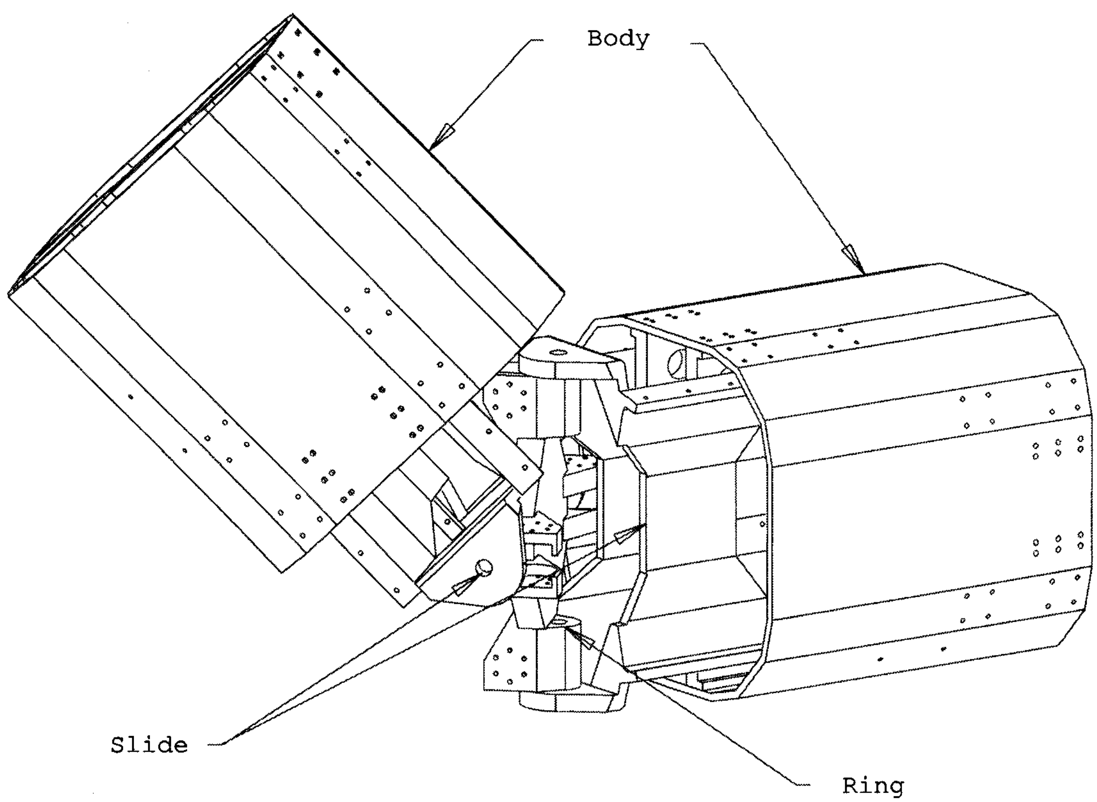

Figure 4.3 Segment assembly.

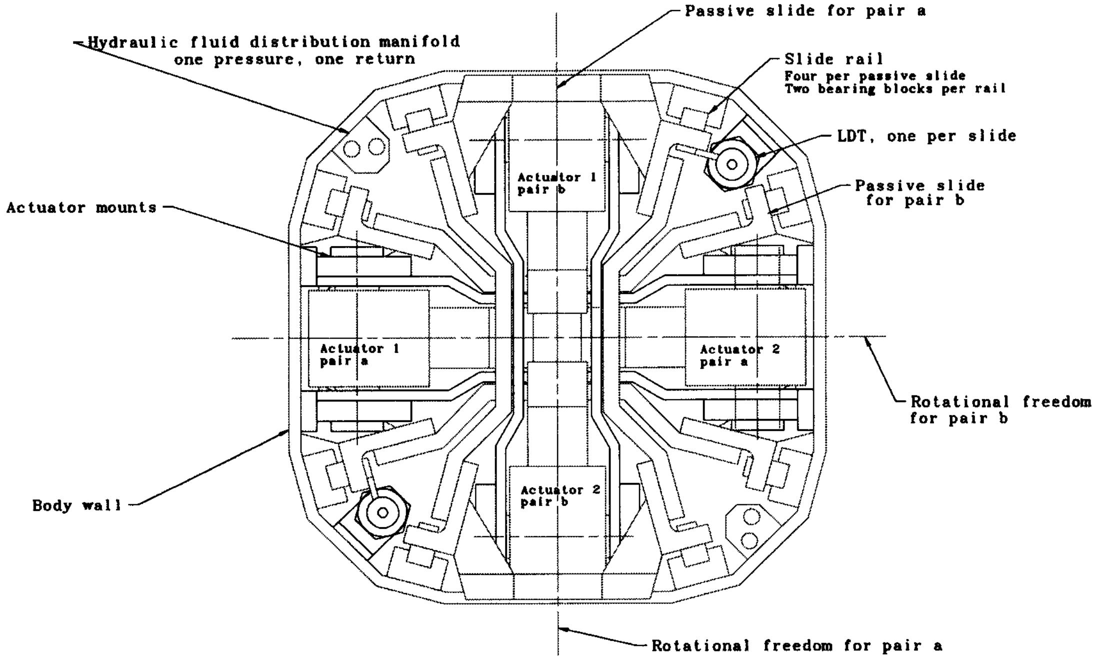

Figure 4.4 ATMS segment section layout.

aluminum mounting bosses. Initial prototyping was performed with a fiberglass-vinyl ester composite to develop the manufacturing process. The principal mechanical components of the design revision are fabricated from a carbon fiber - vinyl ester composite. The carbon fiber utilized is Hercules IM7, an intermediate modulus high strength fiber. The fiber is woven into a 5 harness satin weave fabric by the supplier. The manufacturing process impregnates the dry carbon fabric with catalyzed vinyl ester resin and molds the resulting composite to the desired shape. The ultimate tensile strength of the IM7 fiber is approximately 720,000 psi. The tensile modulus is between 38 and 42 million psi. The strain at failure is 1.7%. The strain at failure is of importance because it determines impact resistance, a weakness of carbon fiber composites. IM7's strain at failure is relatively high when compared with other commercially available carbon fibers. The resulting composite fabricated has an estimated ultimate tensile strength of 75,000 psi and an estimated tensile modulus of 8 million psi.

Several of the parts manufactured include metal inserts that allow mechanical fasteners to be used for assembly and that facilitate joint motion between components. Bearing surfaces are of bronze and are simply inserted in the wet composite during fabrication. Mechanical fastening bosses are aluminum and are inserted in the wet composite during fabrication and then pinned into the composite with shear pins. The shear pins carry the majority of the interfacial loading between the aluminum and the composite so that the adhesive bond is not critical.

A fabrication process for the external structure, or body, has been developed. Four of these tubes have been fabricated from carbon fiber and vinyl ester composite. The mounting holes for the slide bearing blocks, the hydraulic manifolds, the actuators, and the proposed wheels are molded into the body. Figure 4.5 shows the body. The body is a

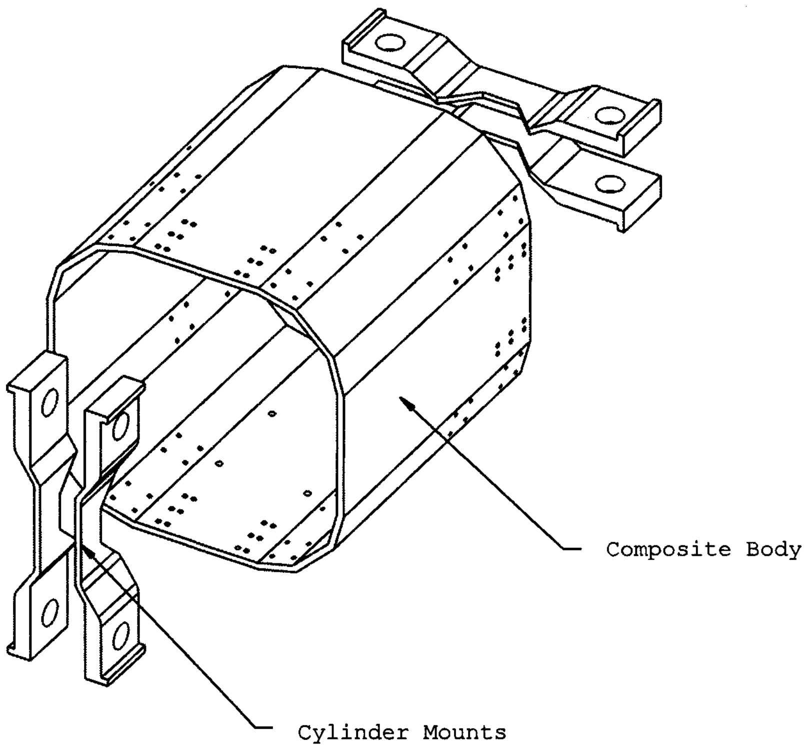

Figure 4.5 Body and actuator mounts.

16 sided tube. The molded-in holes have random E glass chopped mat placed in the laminate to improve elastic response to stress concentrations. This, along with carbon fibers displaced by the hole molding procedure, result in local increases in thicknesses near holes. The body was modeled utilizing finite element analysis. The loads and restraints were applied in a manner similar to that detailed in Chapter 3.2, with the actuator loading increased to 5200 lbs. This increase was due to the reduced area of the rod

increasing actuator pull force. The material data set was generated based on the estimated properties of the composite chosen. Figure 4.6 depicts some results of the deflection analysis. The loads used modeled a worst case condition of maximum joint torque and reaction moment applied on the structure of the segment. Units are in inches. The deflection is shown as approximately 10% of the width of the figure.

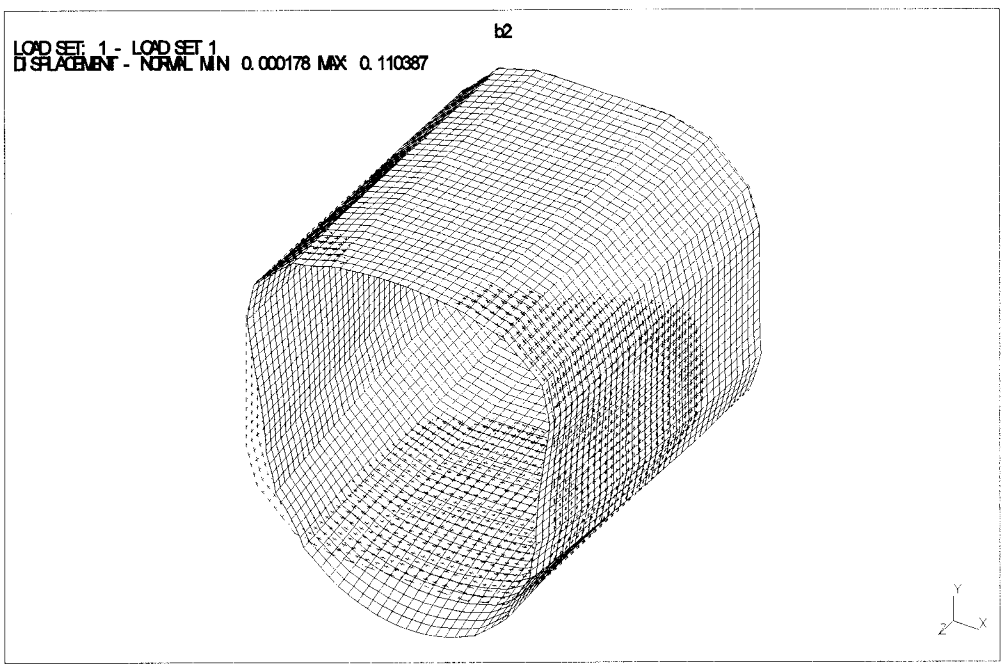

Figure 4.6 Deformation of loaded ATMS segment body.

The cylinder mounts fix the hydraulic actuators to the body. They provide a bearing surface for the trunion of the actuator and a threaded aluminum insert that allows the actuator mounts to be fixed to the body by threaded fasteners. The actuator mounts are illustrated in Figure 4.5. Incorporation of the aluminum insert required the development of a fabrication method that results in both an adhesive and mechanical joint between the carbon fiber composite and the aluminum insert. This was accomplished by incorporating pins fixed in both the insert and the composite oriented in such a way as to transmit a shear load between the insert and the composite. The pin's size is held small to reduce fabrication difficulties with fiber bunching.

The ring component only existed conceptually in the first prototype segment. The first prototype segment was attached to a loading beam and a test stand, not to another segment. Substantial work has been done in designing a rigid connection that does not interfere with the slides or bodies it is attached to. Figure 4.7 illustrates the ring design for the ATMS revision. It is to be constructed primarily of graphite fiber reinforced plastic. The ring has not been fabricated. It remains as future work. All other structural components have been fabricated. Figure 4.8 depicts a digital photographic representation of a segment body with one pair of slides inserted. The

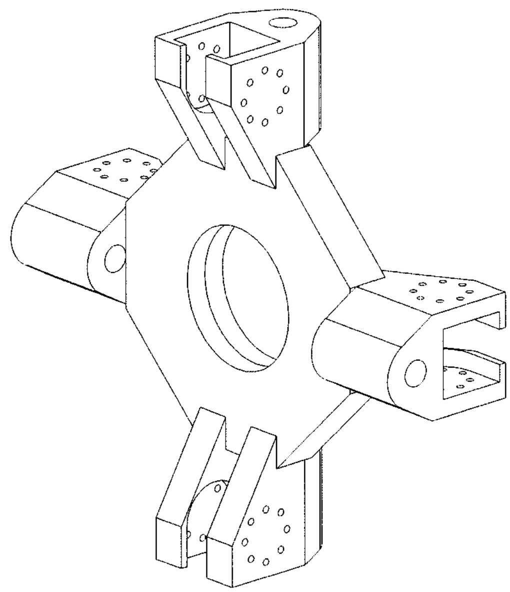

Figure 4.7 ATMS ring design.

mechanical fasteners utilized to joint the slide can be seen. The mechanical fasteners that attach the linear bearing blocks to the body are visible also.

4.3 Expected Performance

Joint torque performance is expected to be slightly better for the second segment design than for the first segment because the rod is smaller, allowing a larger pull force to be generated. The maximum segment length is approximately 44 inches. Table 4.1 lists weights for the second design's components. This leads to a weight per unit

Figure 4.8 Segment body and slide assembly.

length of 4.3 lbs. per inch. This requires a joint torque of 44,580 in.-lbs. to meet the vertical navigation performance requirement of bridging a 12 foot gap. The PPA specified is capable of generating this joint torque for a significant portion of its workspace (Figures 4.1 and 4.2).

Table 4.1 ATMS composite prototype segment weight.

Part	Quantity	Weight each, lbs.	Weight Total, lbs.
Body	1	24	24
Cylinder	4	25	100
Slide Assembly	2	25	50
Ring (estimate)	1	10	10
Misc (encoder, hose, etc)	1	6	6
Total			190

CHAPTER 5
CONCLUSIONS

5.1 Observations and Conclusions

A design methodology is presented for developing the mechanical design of a novel parallel actuation scheme for an articulated mobile robot. The methodology begins by defining the characteristics of the actuation concept and identifying the parameters that define the functionality of the mechanism. Relationships between these mechanism parameters and requirements associated with the application are developed. This process establishes goals for the mechanism parameters. Component variables are defined based on their relationship to the mechanism parameters. These component variables describe the physical implementation of a mechanism that should meet the performance requirements of the application.

This process has been applied to the development of a joint actuation scheme for an Articulated Transporter/Manipulator System. One and a half hardware iterations have been performed. Observations of the performance of the implemented designs are found in Chapter

3.3 and Chapter 4.3. The first prototype exhibited performance that was predictable. The prototype was developed as a test bed for examining the control of a PPA mechanism and for evaluating the implementation difficulty. The prototype met these goals.

The second hardware iteration, partially complete, is intended to provide a serial chain of PPA's oriented in the same plane for use as a test bed in developing. multi-segment control and navigational schemes.

5.2 Future Work

The design methodology is developed. The implantation of the PPA scheme in an articulated robot leaves much to be done. The second mechanical iteration is almost complete. The ring is the last significant structural part that needs developed. After the hardware is complete, navigation and control schemes have to be implemented and evaluated.

APPENDIX
PPA STATICS

The statics of the PPA are useful in evaluating candidate geometries, in component selection, and in structural design. The principal concern is joint torque. A free body diagram of link BC from Figure 2.3 allows the determination of joint torque and bearing reactions if loads are known. Figure A.1 illustrates a free body diagram of link BC.

Several assumptions are made that simplify this analysis. They are noted when made. The following nomenclature will be utilized to develop the statics of link BC.

U_{XY}	Position vector from point Y to point X.
u_{XY}	Unit vector along U_{XY}.
$\lvert U_{XY} \rvert$	Length of position vector U_{XY}.
i	A unit vector directed along the x axis.
j	A unit vector directed along the y axis.
k	A unit vector directed along the z axis.
F_{XY}	Force applied along U_{XY}.

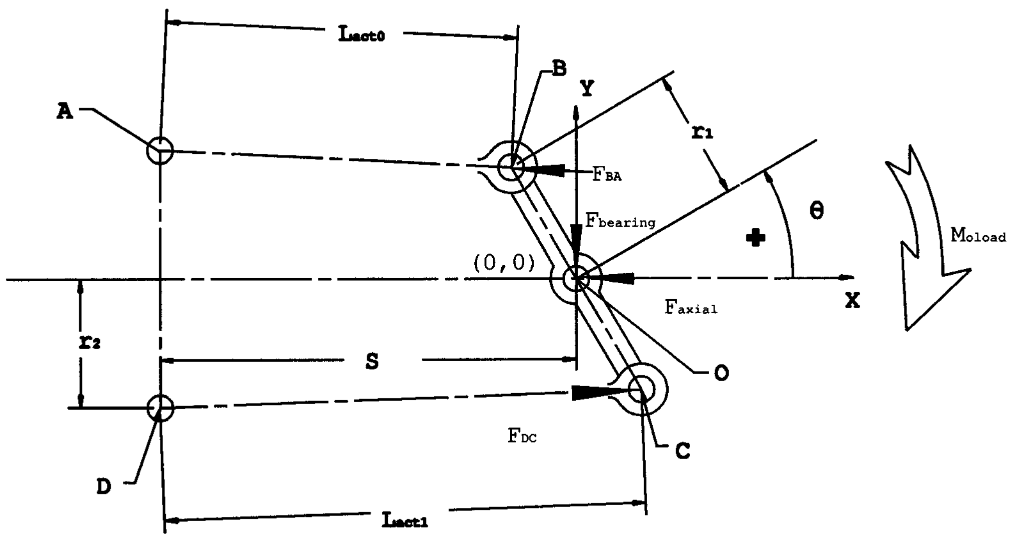

Figure A.1 Free body diagram of link BC.

Position vectors from the origin to the points A, B, C, and D in terms of θ, S, r_1, and r_2 are as follows:

$$U_{AO} = -Si + r_2j$$

$$U_{BO} = -r_1\sin\theta i + r_1\cos\theta j$$

$$U_{CO} = r_1\sin\theta i - r_1\cos\theta j$$

$$U_{DO} = -Si - r_2j$$

The actuator L_{act0} applies a force F_{AB} on link BC along the vector U_{AB} when the actuator is applying a tensile force. The actuator L_{act1} applies a force F_{DC} on link BC along the vector U_{DC} when the actuator is applying a tensile force. If the actuator is pushing instead of pulling, the direction of the force is reversed. These vectors can be found by vector addition.

For actuators pushing, the lines of action are:

$U_{AB} = U_{AO} - U_{BO} = (-S + r_1\sin\theta)i + (r_2 - r_1\cos\theta)j$ and

$U_{DC} = U_{DO} - U_{CO} = (-S - r_1\sin\theta)i + (-r_2 + r_1\cos\theta)j$.

For actuators pulling, the lines of action are:

$U_{BA} = U_{OA} - U_{OB} = (S - r_1\sin\theta)i + (-r_2 + r_1\cos\theta)j$ and

$U_{CD} = U_{CO} - U_{DO} = (S + r_1\sin\theta)i + (r_2 - r_1\cos\theta)j$.

The forces and moments considered acting on the link BC in the free body diagram are F_{AB}, F_{CD}, F_{axial}, $F_{bearing}$, and M_{Oload}.

$F_{AB} = |F_{AB}|u_{ab}$

$F_{CD} = |F_{cd}|u_{cd}$

$F_{axial} = |F_{axial}|i$

$F_{bearing} = |F_{bearing}|j$ (assumes no friction)

$M_{Oload} = |M_{Oload}|k$

Newton's second law, applied to a body in static equilibrium, can be written as F = 0 where F is a vector sum of all forces and moments acting on the body. In the planar case, this reduces to:

$$F = \sum F_x + \sum F_y + \sum M_O = 0. \tag{A.0}$$

This analysis is for the examination of joint torque generation of a PPA mechanism while it is under large external load. It is the philosophy of the design (and a limit of real-time autonomous control) that this motion be considered quasi-static. Developing the equation and equating each component to zero, functional relationships are developed between θ, S, r_1, and r_2 and joint reactions.

$\sum F_x = 0$

$$\sum F_x = F_{AB} \bullet i + F_{CD} \bullet i + F_{axial} \bullet i = 0 \qquad (A.1)$$

where

$$F_{AB} \cdot i = \frac{|F_{AB}|}{|U_{AB}|}(r_1 \sin\theta - S)$$

$$F_{CD} \cdot i = \frac{|F_{CD}|}{|U_{CD}|}(r_1 \sin\theta + S)$$

$$F_{axial} \cdot i = |F_{axial}| i \quad \textit{by definition}$$

$\sum F_y = 0$

$$\sum F_y = F_{AB} \bullet j + F_{CD} \bullet j + F_{axial} \bullet j + F_{bearing} \bullet j = 0 \qquad (A.2)$$

where

$$F_{AB} \cdot j = \frac{|F_{AB}|}{|U_{AB}|}(r_2 - r_1 \cos\theta)$$

$$F_{CD} \cdot j = \frac{|F_{CD}|}{|U_{CD}|}(r_2 - r_1 \cos\theta)$$

$$F_{axial} \cdot j = 0$$

$$F_{bearing} \cdot j = |F_{bearing}| j$$

For $\sum M_O = 0$, the right handed sense is taken as positive.

$$\sum M_O = F_{AB} \times U_{AO} + F_{CD} \times U_{CO} + F_{axial} \times i + F_{bearing} \times i - M_{Oload} = 0 \quad (A.3)$$

where

$$F_{AB} \times U_{AO} = \frac{|F_{AB}|}{|U_{AB}|}(r_1(r_2 \sin\theta - s\cos\theta))k$$

$$F_{CD} \times U_{CO} = -\frac{|F_{CD}|}{|U_{CD}|}(r_1(r_2 \sin\theta + S\cos\theta))k$$

$$F_{axial} \times i = 0$$

$$F_{bearing} \times j = 0.$$

Equations A.1, A.2, and A.3 represent the statics of link BC. Equation A.1 establishes a relationship between actuator forces and axial load. If the axial loading condition is known, then the actuator forces are related to each other by:

$$|F_{AB}| = -\frac{|U_{AB}|}{|U_{CD}|}\,\frac{(r_1\sin\theta + S)}{(r_1\sin\theta - S)}|F_{CD}| - \frac{|U_{AB}|}{(r_1\sin\theta - S)}|F_{axial}| \qquad (A.4).$$

This expression, used in conjunction with maximum actuator force capacity, can be used to establish each actuator force. An actuator is capable of generating a limited force, so equation A.4 must be evaluated so that calculated actuator force is within the capacity of the actuator. Equation A.4 couples slide load with torque. After actuator forces are known, equation A.2 can be used to determine bearing load and equation A.3 can be used to examine the relationship between actuator force and joint torque.

The determination of the bearing load involves solving A.2 for $F_{bearing}$. This solution is represented in A.5.

$$F_{bearing} = -\frac{|F_{AB}|}{|U_{AB}|}(r_2 - r_1\cos\theta) \;-\; \frac{|F_{CD}|}{|U_{CD}|}(r_2 - r_1\cos\theta) \qquad (A.5).$$

This equation neglects the weight of the link, considered small with respect to the moment load that generates the majority of the bearing reaction. It also assumes a frictionless joint, allowing all of the reaction to act along the j vector.

The joint torque that can be generated for a joint in static equilibrium is developed in equation A.6 by solving equation A.3 for M_{Oload}. Equation A.3 reduces to:

$$M_{Oload} = F_{AB} \times U_{AO} + F_{CD} \times U_{CO} \qquad (A.6).$$

with $F_{AB} \times U_{AO}$ and $F_{CD} \times U_{CO}$ defined above. M_{Oload} is taken to act in a negative sense on link BC. The actuator forces are taken to apply a positive moment to link BC.

LIST OF REFERENCES

Askeland, Donald R. The Science and Engineering of Materials, PWS Publishers, Boston, MA, 1984, pp 531.

Clough, Roger L., Gillen, Kenneth T., and Dole, M., International Encyclopedia of Composites, VCH Publishers, New York, NY, 1991, vol. 5 pp 14.

Crane, C., Chaing, S.C., Tulenko, J., and Carlton, R., "Algorithm Development and Computer Graphics Simulation of an Articulated Transporter/Manipulator System", ASME Computers in Engineering Conference, San Francisco, CA, July 1988, vol. 2, pp 253-257.

Hirose, S. and Morishima, A. "Design and Control of a Mobile Robot with an Articulated Body", The International Journal of Robotics Research, April 1990, vol. 9, No 2, pp 99-114.

Hirose, S. and Umetani, Y. "An Active Cord Mechanism with oblique Swivel Joints and its Control", 4th Symposium on Theory and Practice of Robots and Manipulators Proceedings, Zaborow, Poland, 1981, pp 327-340.

Keith, T. G., "Journal Bearings", Standard handbook of Machine Design, McGraw-Hill Book Company, New York, NY, 1986, pp 28.13-28.14.

Lewis, M. A., and Zehnpfennig, D. M., "A Snake-Like Robot for 3-D Visual Inspection", IEEE International Conference on Intelligent Robots and Systems, Munich, Germany, 1994 vol. 2 pp 1310-1317

Merritt, H. Hydraulic Control Systems, John Wiley and Sons, New York, NY, 1967, pp 227.

Milkovich, S. M., Herakovich, C. T., and Sykes, G. F., "Space Radiation Effects on the Thermo-Mechanical Behavior of Graphite-epoxy Composites", Environmental Effects on Composites, 1988, vol. 3, pp 141.

Ridgeway, S., Crane, C., Adsit, P., and Harrell, R., "The Mechanical Design of a Parallel Actuated Joint for an Articulated Mobile Robot", ASME Mechanisms Conference, Scottsdale, AZ, September 1992, vol. 45, pp 591.

Spotts, M. F., Design of Machine Elements, Prentice-Hall, Inc., Englewood Cliffs, New Jersey, 1985, pp 435.